

# Regional seismic stratigraphic framework and depositional history of the post-Valanginian passive margin sequences in the Northern Carnarvon Basin, North West Shelf of Australia

Mulky Winata<sup>a,b,\*</sup>, Chris Elders<sup>a</sup>, Vittorio Maselli<sup>c</sup>, Randell A. Stephenson<sup>b</sup>

<sup>a</sup> School of Earth and Planetary Sciences, Faculty of Science and Engineering, Curtin University, Kent Street, Bentley, Perth, WA, 6102, Australia

<sup>b</sup> School of Geosciences, University of Aberdeen, Meston Building, King's College, Aberdeen, AB24 3UE, United Kingdom

<sup>c</sup> Department of Earth and Environmental Sciences, Life Sciences Centre, Dalhousie University, 1459 Oxford Street, Canada

## ARTICLE INFO

### Keywords:

Seismic stratigraphy  
Seismic facies  
Bottom current  
Mass transport complexes  
Deep water sediments  
Passive margin  
Northern carnarvon basin  
Exmouth plateau  
North west shelf Australia

## ABSTRACT

The post-rift succession of the Northern Carnarvon Basin (north-western Australia) has commonly been interpreted as a relatively simple and uniform sequence that records a transition from siliciclastic to carbonate sedimentation deposited on a passive margin. However, given the significant vertical and lateral variation in seismic facies visible on seismic data, this interpretation likely oversimplifies the depositional history of the margin. Regional composite seismic lines that cross most of the basin, integrated with lithological and biostratigraphic information from exploration wells, provide the context for a better understanding of the depositional processes and environments that characterize the post-rift continental margin succession. We show that the sedimentary sequences deposited above the Valanginian breakup unconformity contain a wide variety of seismic facies that can be linked to a number of different marine depositional environments, with the greatest lateral variation occurring in the Turonian – Rupelian and in the Tortonian – Present. The former interval consists of three dominant seismic facies, namely polygonally faulted, incised, and parallel bedded, which we interpret to indicate a lateral transition from an environment primarily dominated by fine-grained pelagic/hemipelagic deposition to one dominated by energetic bottom currents that created both depositional and erosional features, such as contourite drifts and associated moats. The latter interval is expressed by sigmoidal and continuous reflections which pass laterally into more chaotic reflection packages, which we interpret as clinofolds and mass-transport complexes (MTCs). The development of bottom currents may be connected to changes in circulation associated with the opening of oceans adjacent to the northwest margin of Australia, while the MTCs may indicate increased regional seismic activity and slope instability resulting from the development of collisional plate boundaries. Definition of these sequences highlights the significant changes that have occurred in the sedimentary processes that operated on the margin, and their potential link to its tectonic evolution.

## 1. Introduction

The Northern Carnarvon Basin (NCB) is a large sedimentary basin located in the southernmost part of the North West Shelf (NWS) of Australia (Fig. 1a and c). It is a prolific hydrocarbon basin with most of the plays, including source rocks and reservoirs, deposited during different phases of rifting between the Triassic and the Early Cretaceous (Geoscience Australia, 2015). Consequently, a large number of studies have investigated the syn-rift geological history of the basin (AGSO

North West Shelf Study Group, 1996; Longley et al., 2002; Norvick, 2002; Jablonski and Saitta, 2004; Marshall and Lang, 2013). By comparison, relatively little is known about the post-rift sedimentary sequences deposited in Late Mesozoic and Cenozoic times. This knowledge gap is due to several factors that include: 1) limited and non-economic hydrocarbon prospectivity of the post-rift sequence, 2) limited availability of scientific and commercial boreholes with recovery in post-rift sequences, and 3) uncertainties in the regional correlation of depositional sequences due to variable local lithostratigraphic schemes and the

\* Corresponding author. School of Earth and Planetary Sciences, Faculty of Science and Engineering, Curtin University, Kent Street, Bentley, Perth, WA, 6102, Australia.

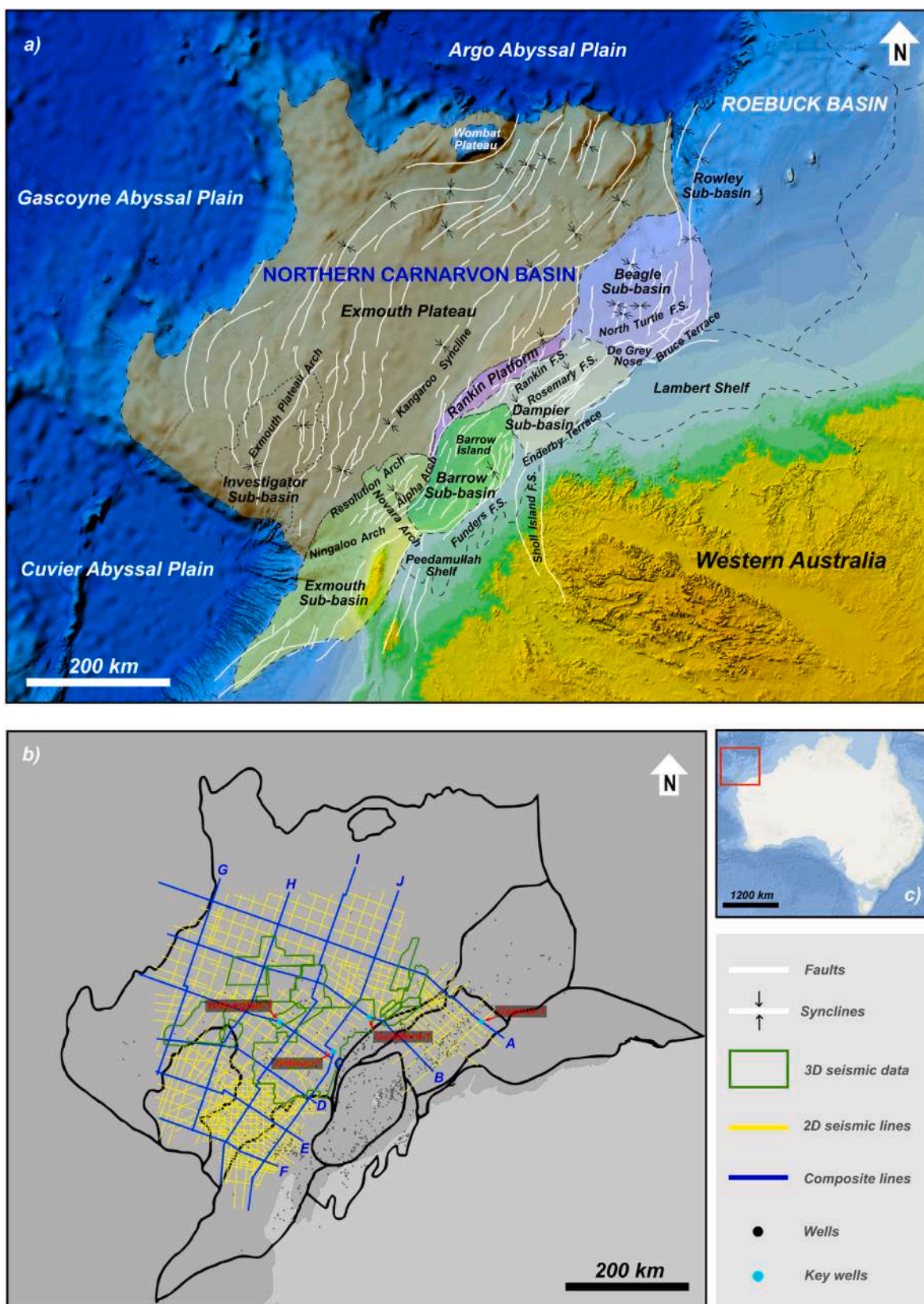
E-mail addresses: [mulky.winata@postgrad.curtin.edu.au](mailto:mulky.winata@postgrad.curtin.edu.au) (M. Winata), [chris.elders@curtin.edu.au](mailto:chris.elders@curtin.edu.au) (C. Elders), [vittorio.maselli@dal.ca](mailto:vittorio.maselli@dal.ca) (V. Maselli), [r.stephenson@abdn.ac.uk](mailto:r.stephenson@abdn.ac.uk) (R.A. Stephenson).

<https://doi.org/10.1016/j.marpetgeo.2023.106418>

Received 1 February 2023; Received in revised form 13 July 2023; Accepted 15 July 2023

Available online 27 July 2023

0264-8172/© 2023 The Authors. Published by Elsevier Ltd. This is an open access article under the CC BY-NC license (<http://creativecommons.org/licenses/by-nc/4.0/>).



**Fig. 1.** a) Location map illustrating geological provinces and structural elements of the Northern Carnarvon Basin (modified from Geoscience Australia, 2015). b) Ten regional lines were constructed from 2D & 3D seismic data, tied to 40 wells distributed along and close to the lines. The interpreted horizons were tied to Cygnus-1, Guilford-1, Yellowglen-1 and Orthrus-1 to assign biostratigraphic ages. c) The NCB is part of North West Shelf of Australia Basins (red square).

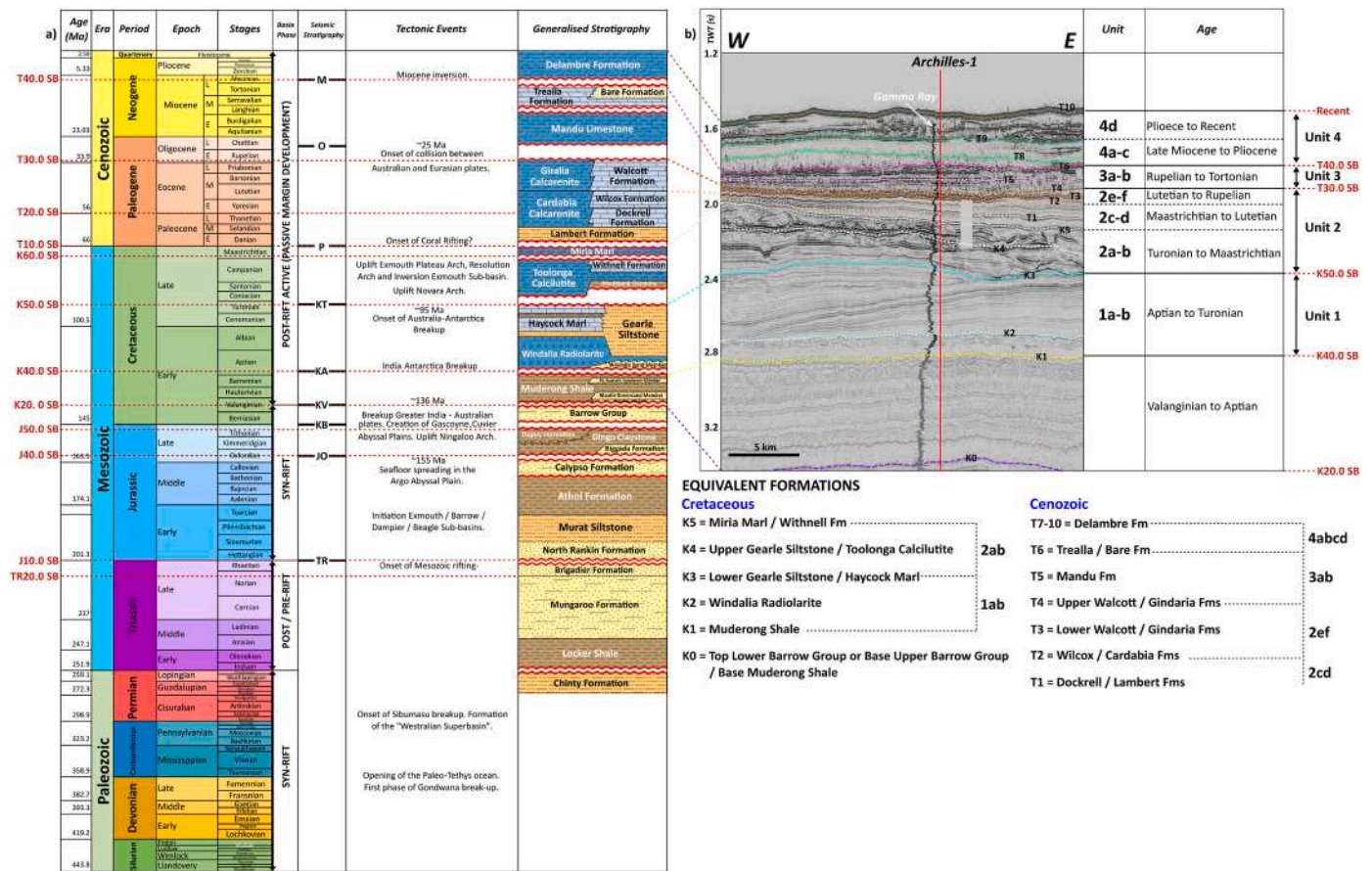


Fig. 2. a) Generalised tectono-stratigraphic chart in the NCB (tectonic events and stratigraphy compiled from Romine et al., 1997; Jablonski, 1997; Longley et al., 2002; Cathro and Karner, 2006; Gibbons et al., 2012; Marshall and Lang, 2013; Geoscience Australia, 2015; Gartrell et al., 2016; Paumard et al., 2018). Formation names and lithostratigraphic terms are used according to the Australian Stratigraphic Units Database. Red dashed lines are boundaries that given by Marshall and Lang (2013). b) Seismic stratigraphic nomenclature in the NCB. The Birdrong Sandstone/Zeepard Fm are recognised as the Upper Barrow Group. Fm/Fms: Formation(s).

presence of a large number of unconformities. Although regionally correlatable sequence stratigraphic boundaries have been identified (Marshall and Lang, 2013), this still leaves open many questions regarding the post-rift depositional history of the basin and the main processes driving sediment accumulation on the passive margin.

Recently acquired seismic data reveal the complexity of the post-rift interval, which is in contrast with existing, and often relatively simple, lithostratigraphic schemes (Geoscience Australia, 2015; well reports). Utilising regional 2D and 3D seismic reflection surveys integrated with well data, we investigate the lateral and vertical variation in seismic facies within and between previously recognised sequence stratigraphic boundaries to propose a seismic stratigraphic framework that accounts for the depositional environments and their spatial and temporal changes across the margin. The widespread availability of high quality seismic data and the variability of seismic facies makes the North West Shelf an excellent location to investigate the complexity of the sedimentary processes that operated on the deeper part of the continental margin and insights gained from this margin may be applied to other continental margins in similar settings.

## 2. Tectono-stratigraphic setting

The NCB lies at the southwest end of the NWS of Australia. It covers an area that encompasses the present-day shelf to the deep-water segment of the Exmouth Plateau (Fig. 1a), as far as the limit between the continental slope and the abyssal plain. The basin is divided into several sub-basins including the Exmouth, Barrow, Dampier and Beagle

sub-basins (Fig. 1a), which contain Mesozoic and Cenozoic sequences that are more than 15 km thick (Bradshaw et al., 1988; Gartrell, 2000; Longley et al., 2002). The Exmouth Plateau is an area of distributed extensional faults that developed from the basin flanks to the edge of the abyssal plain (Fig. 1a; Falvey and Veivers, 1974; Exon and Willcox, 1978; Barber, 1988; Scarselli et al., 2013). The NWS underwent a complicated tectono-stratigraphic evolution from the Late Paleozoic to Cenozoic associated with the breakup and separation of Gondwana (Audley-Charles et al., 1988; Bradshaw et al., 1988; Stagg and Colwell, 1994; Driscoll and Karner, 1998; Borel and Stampfli, 2002; Metcalfe, 2013; Reeve et al., 2016; Paumard et al., 2018). In the Late Permian to Triassic, following Permian extension, a large part of the basin was in the post-rift phase, predominantly characterised by thermal subsidence. The first phase of Mesozoic rifting occurred during the Late Triassic to Early Jurassic, resulting in the formation of sub-basins (Barber, 1988; Marshall and Lang, 2013; Paumard et al., 2018). During the middle Jurassic, the basin moved into the main rifting phase (Jablonski, 1997), which in some places extended into the late Jurassic, culminating in Valanginian breakup between India and Australia (Etheridge and O'Brien, 1994).

The breakup led to the formation of a regionally recognised unconformity and correlative disconformity (the Valanginian Unconformity (Fig. 2), or K20.0 SB of Marshall and Lang, 2013) which is only locally associated with uplift and erosion (Tindale et al., 1998), such as that which formed the Ningaloo Arch (Fig. 1a; Tindale et al., 1998; Longley et al., 2002; Heine and Müller, 2005; Gibbons et al., 2012). A product of the erosion was the deposition of a deltaic sequence, identified as the

**Table 1**

a) Ten regional composite lines composed of 22 seismic vintages in the area of interest. Lines A-F trend WNW-ESE and lines G-J trend SSW-NNE. b) 2D seismic surveys used for the regional interpretation were acquired and processed in the 1990s and 2000s. The information was compiled from the WAPIMS website (Western Australian Petroleum and Geothermal Information Management System). NA is information not available. c) 3D seismic surveys used in this study were acquired and processed in the 1990s and 2000s. The information was compiled from the WAPIMS website (Western Australian Petroleum and Geothermal Information Management System). NA is information not available.

Line	Seismic Survey						~ Total km in AOI	Direction
A	EX00-29, 98C-4143, 98C-4134, Xline 5047 Banambu 3D, PG93-1040, PG93-1009, GPDB95-03						588.667	WNW - ESE
B	EX00-15, Random line Centaur 3D, B02-35 M, 98C-4083, 98C-4090, Xline 1209 Rosie 3D, Random line SW Rankin 3D, GPDB95-14					465.116		
C	EX00-01, EX00-28, B02-44 M, JA95-115					327.144		
D	X79B-1129, X79B-1100, HE94-230, JA95-220, JA95-108 E, EX08-010 M, EX05-011					269.168		
E	EX05-023, EX05-065, HE94-150, HE96-22					252.547		
F	98J-4169, HE94-104, EX05-043					199.812		
G	OM08-602, OM08-501, EX05-050					318.508	SSW - NNE	
H	EX00-26, JA95-209 N, X95A-2148, X95A-2107, X95A-2127, JA95-209 S, EX05-057					396.686		
I	SK56P-056, HE94-109, HE94-190, HE94-105, HE94-200, JA95-217, JA95-121, B02-65 M, AMAGNAC2D-W08AM-0033, EX00-44, OM08-032, OM08-104					530.515		
J	EX00-60, OM08-111, 98C-4085, JA95-222, JA95-116, Inline 1928 Draeck 3D, WAS76-17, 98J-4155					547.539		

No	Survey name	Survey type	Line prefix	Start date	End date	Operator	Contractor	Line Length (km)
1	Scientific Investigation 10 SL	2D	WAS76	July 29, 1976	September 30, 1976	Geophysical Service Inc	GSI	7708
2	NA	2D	X78A	February 19, 1978	January 02, 1979	Esso Exploration & Production Aust Inc	GSI	17167
3	X79B	2D	X79B	July 07, 1979	September 16, 1979	Esso Exploration & Production Aust Inc	GSI	5570
4	Michelle	2D	PG93	November 12, 1993	December 10, 1993	Phillips Australian Oil Company	WesternGeco	3100.5
5	HE94	2D	HE94	June 20, 1994	August 12, 1994	BHP Petroleum (Australia) Pty Ltd	WesternGeco	6255.1
6	SPA 2SL/1994-95	2D	GPDB95	June 22, 1995	August 27, 1995	WesternGeco Australia Pty Ltd	WesternGeco	2523
7	X95A	2D	X95A	September 27, 1995	October 27, 1995	Esso Australia Pty Ltd	NA	2440.24
8	JA95	2D	JA95	October 13, 1995	December 16, 1995	Japan National Oil Corporation	AGSO	6691.2
9	NA	2D	EXS96	May 30, 1996	June 15, 1996	PGS Nopec Australia Pty Ltd	Nopec	1750
10	HE96	2D	HE96	June 01, 1996	June 15, 1996	BHP Petroleum (Australia) Pty Ltd	Digicon Inc	1766.4
11	Capri	2D	98C	January 31, 1998	March 12, 1998	Woodside Offshore Petroleum Pty Ltd	NA	4702.1
12	Jawa	2D	98 J	March 12, 1998	March 25, 1998	Woodside Offshore Petroleum Pty Ltd	NA	1780.53
13	Exmouth North	2D	EX00	December 19, 1999	June 15, 2000	Australian Seismic Brokers Pty Ltd	Veritas	8446
14	Champagne/Wheatstone	2D	B02	March 20, 2003	April 22, 2003	Chevron Texaco Australia Pty Ltd	Veritas	847.6-2546
15	Klimt	2D	OM08	January 18, 2008	April 29, 2008	OMV Australia Pty Ltd	Gardline Marine	7407
16	Armagnac	2D	NA	June 24, 2008	September 04, 2008	Woodside Burrup Pty Ltd	Veritas	6399
17	NA	2D	EX08	NA	NA	NA	NA	NA
18	NA	2D	EX05	NA	NA	NA	NA	NA
19	NA	2D	SK	NA	NA	NA	NA	NA

No	Survey name	Survey type	Line prefix	Start date	End date	Operator	Contractor	Area (sqkm)
1	South West Rankin	3D	R96	February 20, 1996	April 30, 1996	Woodside Offshore Petroleum Pty Ltd	Western Geophysical Company	783
2	Rosie	3D	RO3	November 19, 1996	February 18, 1997	Western Mining Corporation Ltd	NA	1139
3	Banambu	3D	NA	December 22, 1997	February 02, 1998	Woodside Offshore Petroleum Pty Ltd	NA	1164
4	Chandon	3D	NA	February 19, 2004	April 08, 2004	Chevron Texaco Australia Pty Ltd	NA	1237
5	Scarborough	3D	NA	March 20, 2004	May 09, 2004	BHP Billiton Petroleum (Australia) Pty Ltd	WesternGeco	1266.27
6	Io-Jansz	3D	NA	April 12, 2004	September 19, 2004	Chevron Texaco Australia Pty Ltd	Veritas	2785.5
7	Willem	3D	NA	January 15, 2006	April 18, 2006	Woodside Energy Ltd	Veritas	1832.56
8	Duyfken	3D	NA	May 24, 2006	September 02, 2006	Chevron Australia Pty Ltd	Baker Atlas	3600.285
9	Bonaventure	3D	NA	September 02, 2006	December 15, 2006	Chevron Australia Pty Ltd	WesternGeco	4143.743
10	Charon	3D	NA	July 17, 2007	August 27, 2007	Chevron Australia Pty Ltd	Baker Atlas	1799

(continued on next page)

Table 1 (continued)

No	Survey name	Survey type	Line prefix	Start date	End date	Operator	Contractor	Area (sqkm)
11	Draeck	3D	DR07	December 17, 2006	August 20, 2007	Chevron Australia Pty Ltd	WesternGeco	1231
12	Centaur	3D	NA	August 20, 2007 August 29, 2007	August 20, 2007 November 10, 2007	Chevron (TAPL) Pty Ltd	WesternGeco	79.841 2624
13	Meo-NWS	3D	NA	December 13, 2007	December 27, 2007	MEO Australia Ltd	PGS	258.16
14	Glencoe	3D	NA	December 03, 2007	March 19, 2008	Hess Exploration Australia Pty Ltd	CGG Veritas	4485.4
15	Colombard	3D	NA	March 22, 2008	August 07, 2008	Woodside Energy Ltd	CGG Veritas	3172.68
16	Rose	3D	NA	August 18, 2008	September 30, 2008	Oilex Ltd		1498.5075
17	Aragon	3D	NA	August 11, 2008	November 18, 2008	WestenGeco Australia Pty Ltd	WesternGeco	2928.2566
18	Artemis	3D	NA	March 10, 2009	March 31, 2009	NWS Exploration Pty Ltd	PGS	257.83
19	Cazadores	3D	NA	December 30, 2008	March 24, 2009	Woodside Burrup Pty Ltd	WesternGeco	4551
20	Eendracht	3D	NA	June 09, 2009	September 27, 2009	Fugro Multi Client Services Pty Ltd	NA	3223
				January 27, 2010	June 26, 2010		NA	3630
				July 17, 2010	October 27, 2010		NA	7915

Birdrong Sandstone or Upper Barrow Group (Arditto, 1993). Following this, rapid subsidence and sea level rise coinciding with the onset of seafloor spreading caused regional marine flooding, resulting in deposition of a condensed transgressive glauconitic sandstone (the Mardie Greensand) as well as an extensive marine transgression, which resulted in deposition of the Muderong Shale over most of the Northern Carnarvon Basin (Barber, 1988; AGSO North West Shelf Study Group, 1996; Longley et al., 2002; Norvick, 2002; Marshall and Lang, 2013). Between the Valanginian Unconformity and the Barremian, the Muderong Shale was initially deposited in a partially restricted marine embayment (Longley et al., 2002). During the Barremian, India drifted northward creating more open seaways. This, combined with continued subsidence over the entire North West Shelf (Jablonski and Saitta, 2004) resulted in ongoing deposition of the Muderong Shale until the Aptian in an open marine environment (AGSO North West Shelf Study Group, 1996).

By the Aptian, the separation of India, as well as the onset of the separation of Antarctica from Australia, established unrestricted oceanic circulation around the Indian plate (Longley et al., 2002; Jablonski and Saitta, 2004). This caused upwelling and enhanced the productivity of radiolaria (Ellis, 1987; Longley et al., 2002), leading to deposition of the Windalia Radiolarite (Fig. 2; Bradshaw et al., 1988). From the Turonian to Campanian, Antarctica – Australia breakup continued to develop along the southern margin of Australia (AGSO North West Shelf Study Group, 1996). This has been linked to compression in the NCB (Longley et al., 2002; Norvick, 2002; Jablonski and Saitta, 2004), resulting in uplift and structural inversion in the Exmouth sub-basin expressed by the initiation of the Novara Arch in the early Santonian and the Resolution Arch in the earliest Campanian (Figs. 1a and 2; Tindale et al., 1998). In addition, transpression reactivated pre-existing rift structures and created features such as Barrow Island (Fig. 1b; Bradshaw et al., 1998; Tindale et al., 1998).

During the Cenozoic, sedimentation in the NCB was dominated by progradation of carbonate systems along the length of the margin, which developed in warmer water conditions (Apthorpe, 1988; Romine et al., 1997; Longley et al., 2002; Keep et al., 2007). This allowed the formation of an extensive carbonate shelf which continued to develop until the present day, interrupted during the Paleocene by a period of cool-water carbonate deposition in a shallow marine environment, which resulted in the deposition of the Dockrell Formation (Norvick, 2002). The shelf carbonates pass seawards through slope facies into condensed, deep-water carbonates and marls (Norvick, 2002).

In the earliest Eocene, a brief clastic influx occurred in some areas of northwestern Australia (Pattillo and Nichols, 1990; Whittam et al.,

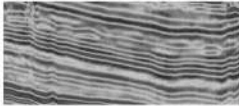
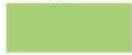
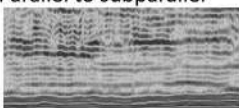

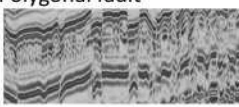


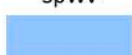
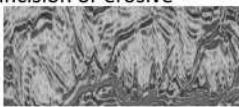
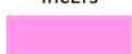


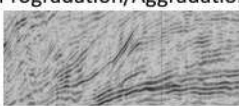
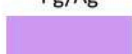


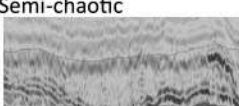

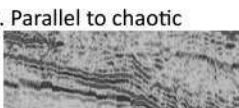

1996). This was followed by further phases of shallow marine carbonate shelf progradation which formed the Giralia Calcarene and Walcott Formation (Norvick, 2002). The progradation of carbonates continued with deposition of the Oligocene to Middle Miocene Mandu Limestone and the Middle Miocene Trealla Limestone (Heath and Apthorpe, 1984; Tindale et al., 1998). In the Miocene, collision of the Australia – India and Eurasia plates contributed to a major compressional event (Longley et al., 2002). This led to inversion in the Late Miocene causing unconformities in the Trealla Limestone and Bare Formation. Carbonate growth in the Trealla Limestone was interrupted by deposition of dolomitic siliciclastic sands of the Bare Formation, which were fed by a delta system (Sanchez et al., 2012; Cathro et al., 2003). The margin remains tectonically active, expressed by the development of the Exmouth Plateau Arch and extensive slope instability, as demonstrated by the widespread development of slides, slumps, mass flows, turbidity currents and debris flows (Jablonski, 1997; Müller et al., 1998; Longley et al., 2002; Cathro and Karner, 2006; Gibbons et al., 2012; Marshall and Lang, 2013; McCormack and McClay, 2013; Scarselli et al., 2013; Gartrell et al., 2016; Paumard et al., 2018). Seismically, these events are clearly captured by contorted and chaotic seismic facies, and some grooves or incisions (Hengesh et al., 2012; Scarselli et al., 2013; Paumard et al., 2019). Widespread mass-transport deposits occur within the Delambre Formation, which was deposited from the Pliocene to Recent (Heath and Apthorpe, 1984; Butcher, 1989).

### 3. Data and methodology

This research uses public domain 2D and 3D seismic reflection and well data that are available from the NOPIMS (National Offshore Petroleum Information Management System) and WAPIMS (Western Australian Petroleum and Geothermal Information Management System) databases (Fig. 1b). Seismic data acquired for petroleum assessment cover almost all the NCB, an area of approximately 139,960 km<sup>2</sup>. 19 2D and 21 3D seismic surveys of different vintages were used for seismic interpretation. The acquisition and processing history of the seismic surveys is summarised in Table 1. In general, pre-stack time-migrated seismic sections provide high-quality images, typically with a 4 ms sampling interval. A mistie correction was applied to each survey by applying a vertical correction factor using the 3D data as a reference. Approximately 40 wells were selected close to seismic lines to provide stratigraphic and lithological constraints on seismic interpretation. It is important to note that the wells mostly targeted Jurassic and Triassic intervals. Consequently, lithological, well log and biostratigraphic data

**Table 2**

Summarised seismic facies description and interpretation for the post-rift NCB explaining the acronyms and the colour legend used in the main text and in the seismic facies maps.

Example	Colour in seismic facies map	Seismic facies	Interpretation
1. Parallel 	Pr 	- Medium to high amplitude - Parallel and laterally continuous	- Laterally continuous deposit - Low energy condition - Distal setting
2. Parallel to subparallel 	PrSp 	- Low to medium amplitude - Parallel to subparallel	(Mitchum et al., 1977a and 1977b)
3. Polygonal fault 	Pf 	- Medium to high amplitude - Semi-continuous - Dissected by faults	- Polygonally faulted deposit - Fine-grained sediment - Low energy condition - Distal setting (Cartwright, 1994 and Watterson et al., 2000)
4. Subparallel to wavy 	SpWv 	- Medium amplitude - Subparallel to wavy	- Small scale bedforms - Moderate bottom current e.g., sediment waves (Stow et al., 2009 and Rebesco et al., 2014)
5. Incision or erosive 	IncErs 	- Low to medium amplitude - Individual to multiple incision(s)	- Erosional surfaces e.g., scours, grooves - Strong bottom current (Hernández-Molina et al., 2003, 2006)
6. Semi- to dis-continuous 	SmcDc 	- Low amplitude - Semi-continuous to discontinuous	- Disturbed deposit - In the inboard area (NCB) - Shelf setting (Mitchum et al., 1977a and 1977b)
7. Progradation/Aggradation 	Pg/Ag 	- Medium to high amplitude - Continuous - Simple to multiple stacked progradation/aggradation	- Cliniforms - Shelf edge to slope (Mitchum et al., 1977a and 1977b)
8. Chaotic to transparent 	Ch 	- Low to medium amplitude - Chaotic	- Slumps and mass transport complexes (MTCs)
9. Semi-chaotic 	SmCh 	- Low to medium amplitude - Semi-continuous to chaotic	- Slope to basinal area
10. Parallel to chaotic 	PrCh 	- Low to medium amplitude - Parallel to chaotic	(Mitchum et al., 1977a and 1977b)

is sparse in the post-Valanginian sequences.

Seismic stratigraphic interpretation was carried out following the principles of Mitchum et al. (1977a, 1977b). Sixteen horizons were selected based on the recognition of unconformities, reflection terminations, prominent seismic characteristics, and lateral continuity. In addition, seismic facies analysis allowed characterisation of their associated units, based on internal reflector geometries, amplitude, and

stacking patterns of reflection sets (Table 2). The interpretation was also controlled by closing loops within the seismic grid to eliminate misties. The horizons were tied to four wells (Cygnus- 1, Guilford-1, Yellowglen-1 and Orthrus-1; Figs. 1b and 3). In addition, thirty-six other wells lying up to 20 km from the lines were used to further constrain the correlation (see well cross-section in Fig. 6). A combination of micro-paleontological and palynological reports from the four wells were used

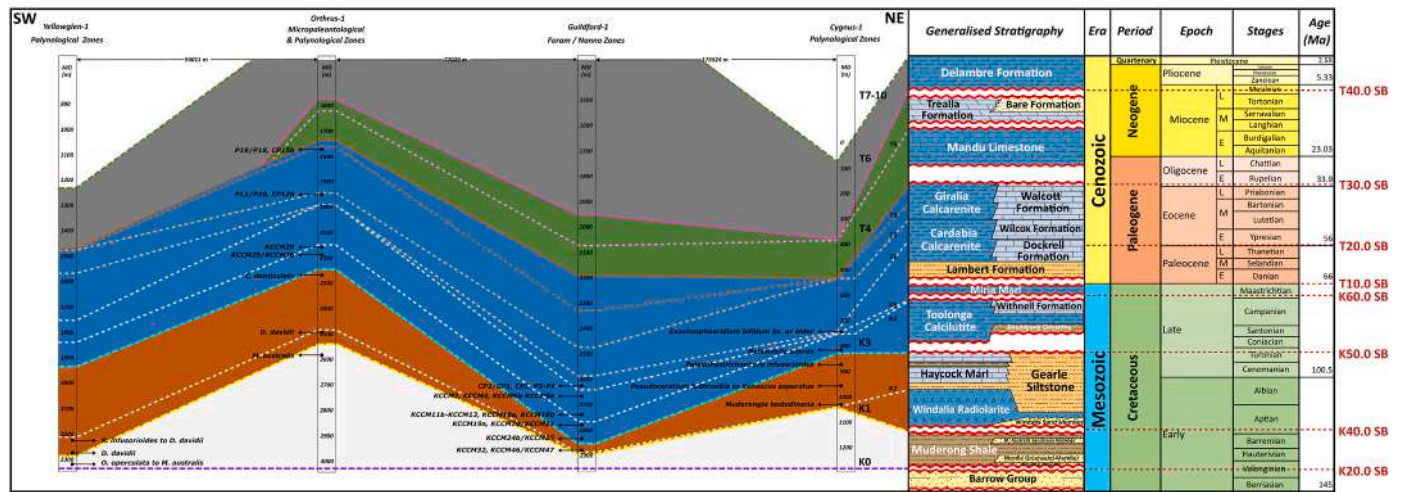


Fig. 3. Stratigraphic ages for the key seismic markers assembled from the Cygnus-1, Guilford-1, Yellowglen-1 and Orthurus-1 well completion reports (see location on Fig. 1b). In addition, units and age intervals in the Neogene are defined and constrained by stratigraphic markers and ditch cuttings descriptions from 36 additional wells. Red dashed lines are boundaries given by Marshall and Lang (2013).

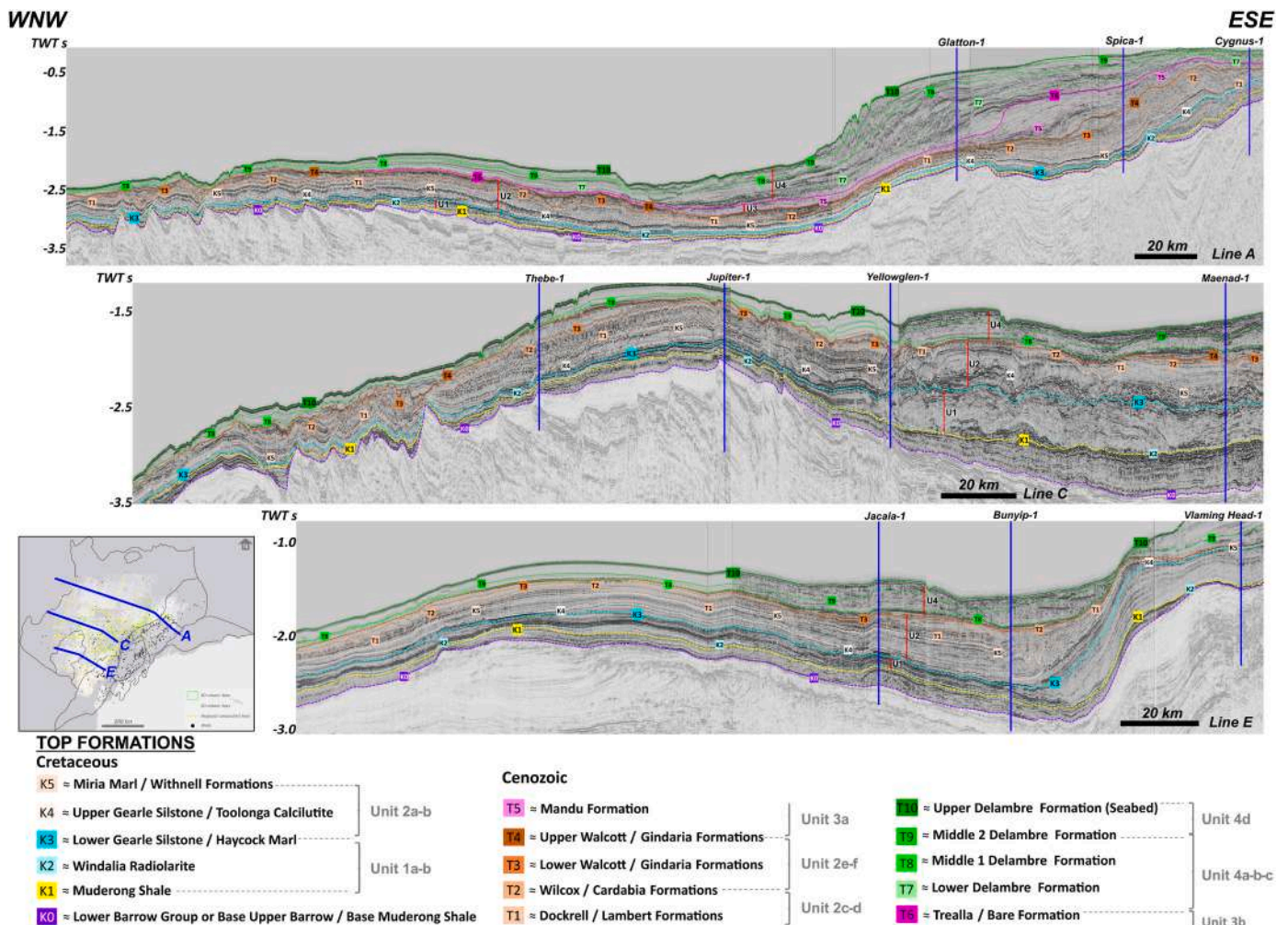


Fig. 4. Seismic stratigraphic interpretation of the NCB shown in seismic lines A, C and E. Sixteen seismic horizons correspond to sixteen formations which can be grouped into four primary units (Units 1–4).

to assign biostratigraphic ages to the interpreted horizons. The horizons are named K0–K5 and T1–T10 using a simple alphanumeric nomenclature, with K corresponding to Cretaceous, T to Cenozoic, and the

numbers representing the age, from old to young (Figs. 2–4). The majority of these horizons are equivalent to the boundaries given by Longley et al. (2002), Marshall and Lang (2013) and Geoscience

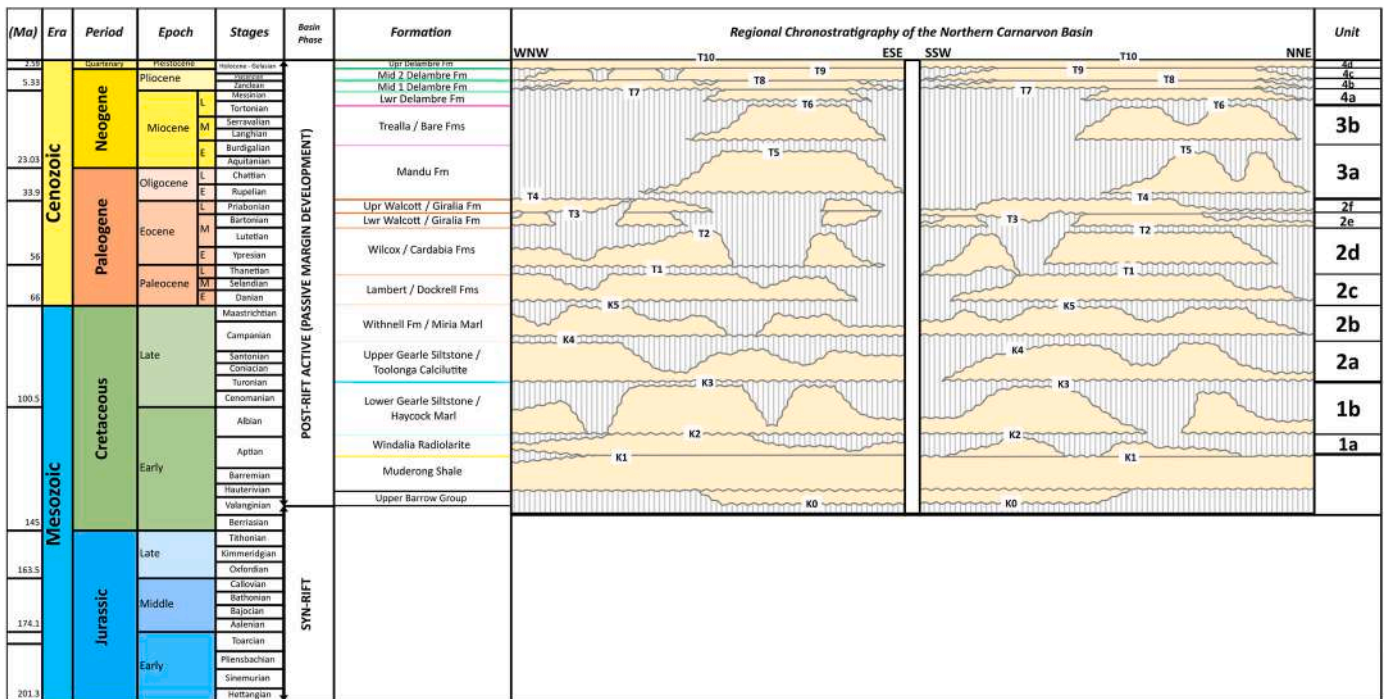


Fig. 5. A summary seismo-chronostratigraphic chart of the post-Valanginian sequences represented on WNW-ESE and SSW-NNE oriented cross-sections.

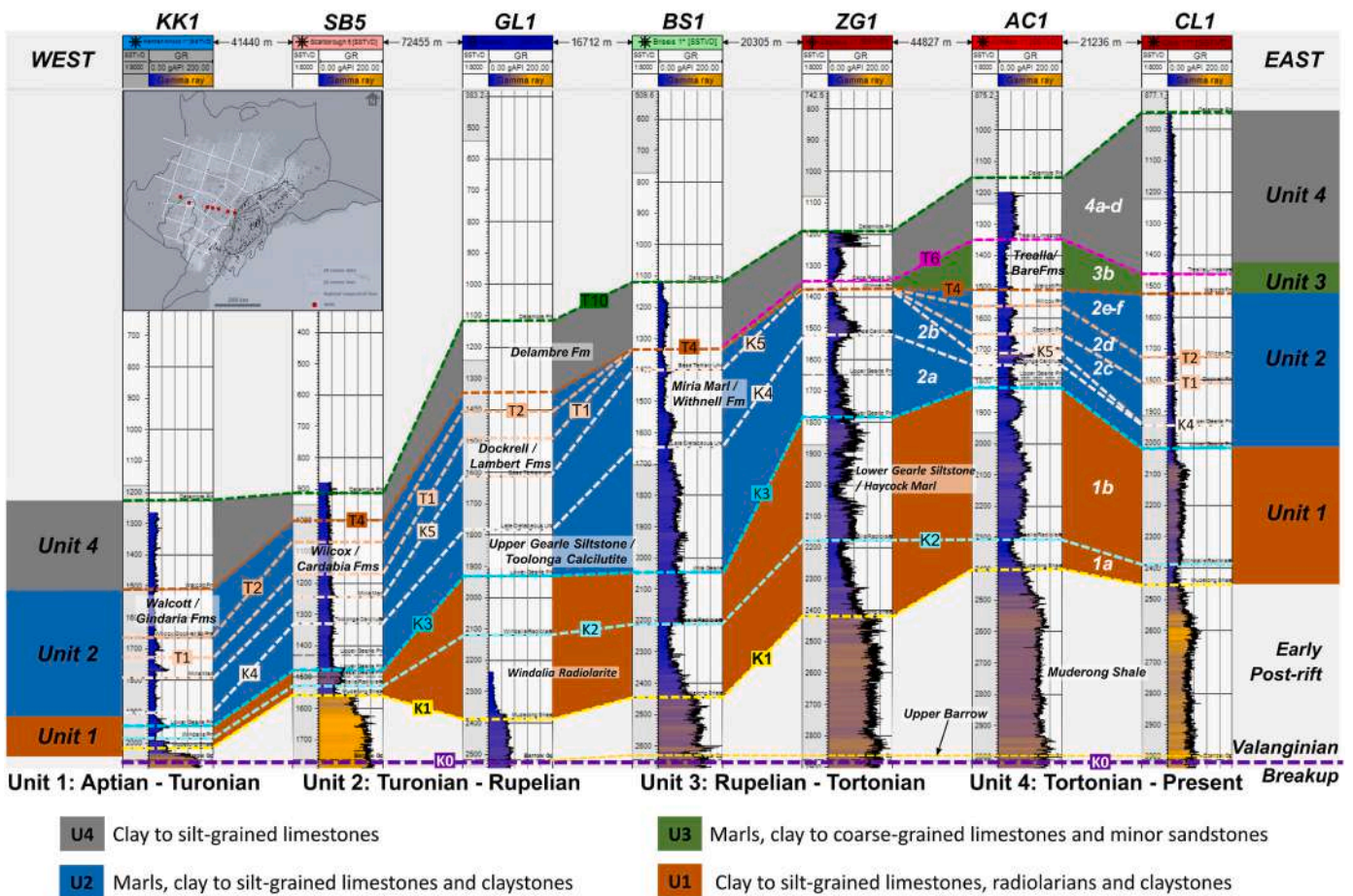


Fig. 6. Well cross-section showing the four main stratigraphic units from west to east in the middle of the Exmouth Plateau. The basal dashed line marks the breakup unconformity and onset of deposition of the Muderong Shale during thermal subsidence. KK1: Kentish Knock-1, SB5: Scarborough-5, GL1: Glenloth-1, BS1: Briseis-1, ZG1: Zagreus-1, AC1: Archilles-1, CL1: Clio.



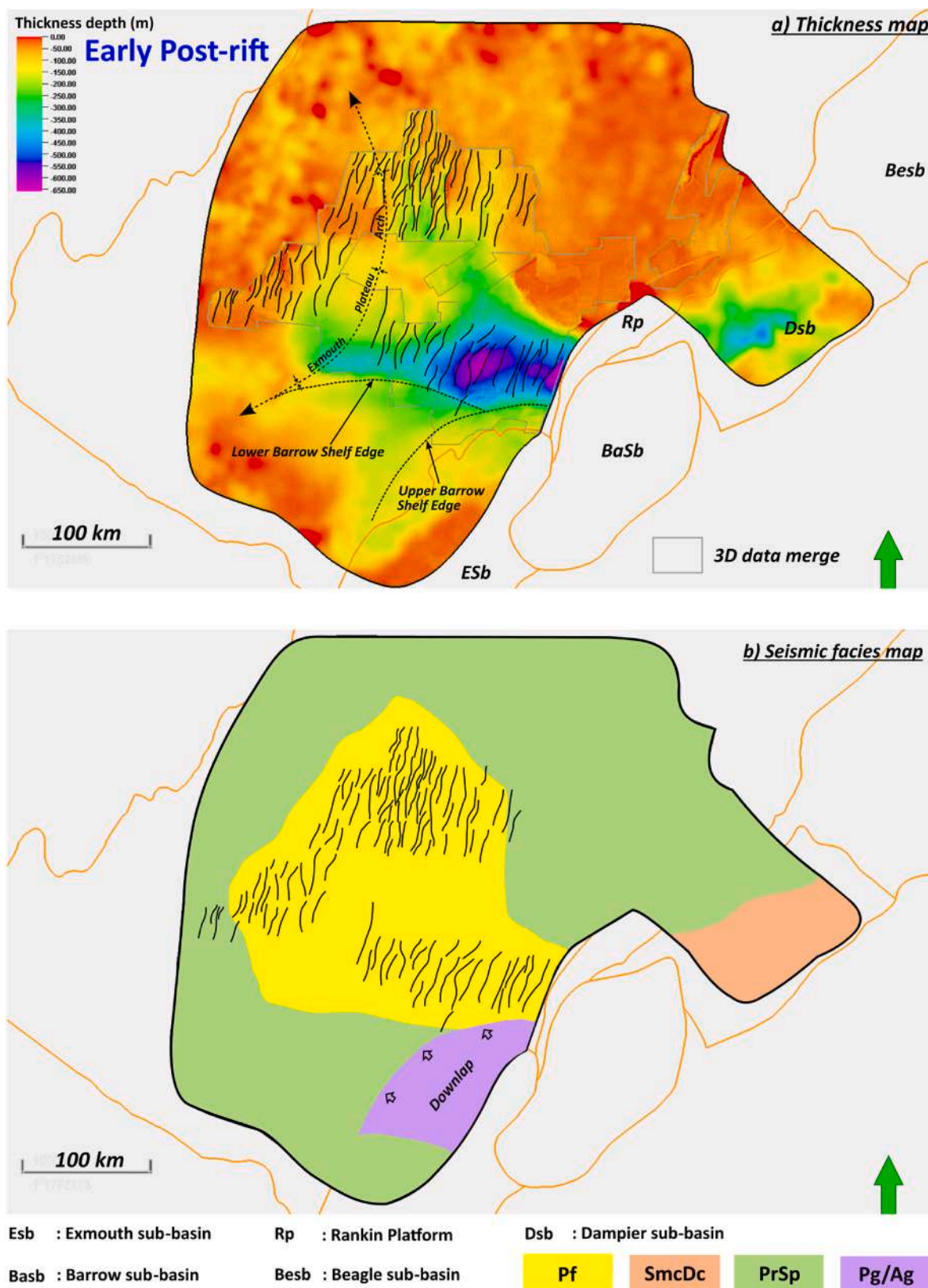
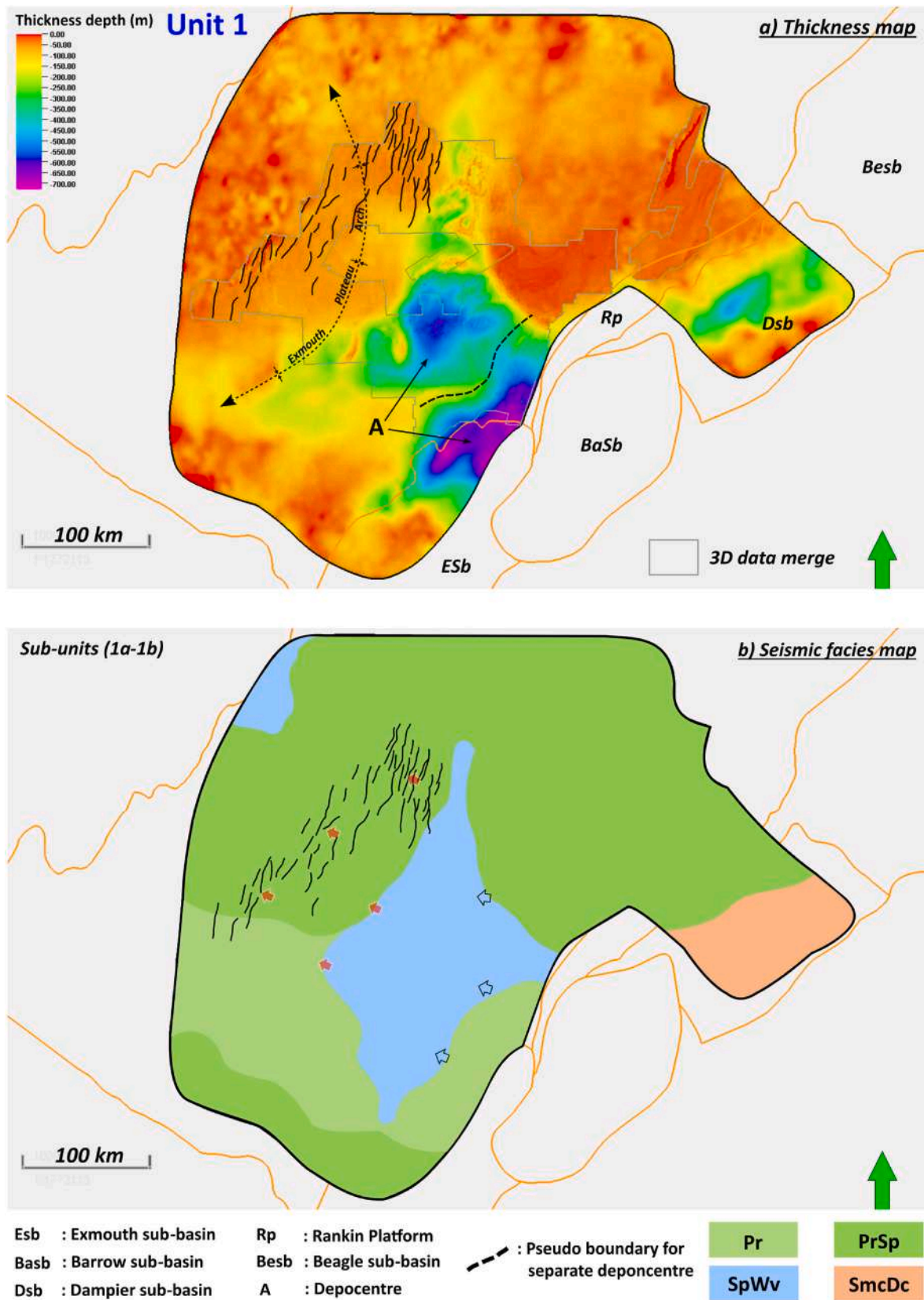


Fig. 7. a) Thickness map of Early Post-rift with sediment depocentre in the middle of the Exmouth Plateau. This map was created from horizons K0 and K1. Black lines indicate the crests of emergent underlying fault blocks. b) Seismic facies map showing that Early Post-rift is mostly characterised by polygonal faulting and parallel to subparallel facies (see Table 2 for colour legend). The Upper Barrow Group is included in the Early Post-rift interval. Pf (Polygonal fault), SmcDc (Semi-to discontinuous), PrSp (Parallel to Subparallel), Pg/Ag (Progradation/Aggradation).



**Fig. 8.** Unit 1 consists of sub-units 1a and 1 b. a) Thickness map of Unit 1 with sediment depocentre A. This map was created from horizons K3 and K1. Black lines indicate the crests of emergent underlying fault blocks. b) Seismic facies map showing that Unit 1 is mostly characterised by parallel and subparallel facies (see Table 2 for colour legend). Red arrow: onlaps, black arrow: downlaps. Pr (Parallel), PrSp (Parallel to Subparallel), SpWv (Subparallel to Wavy), SmcDc (Semi-to discontinuous).

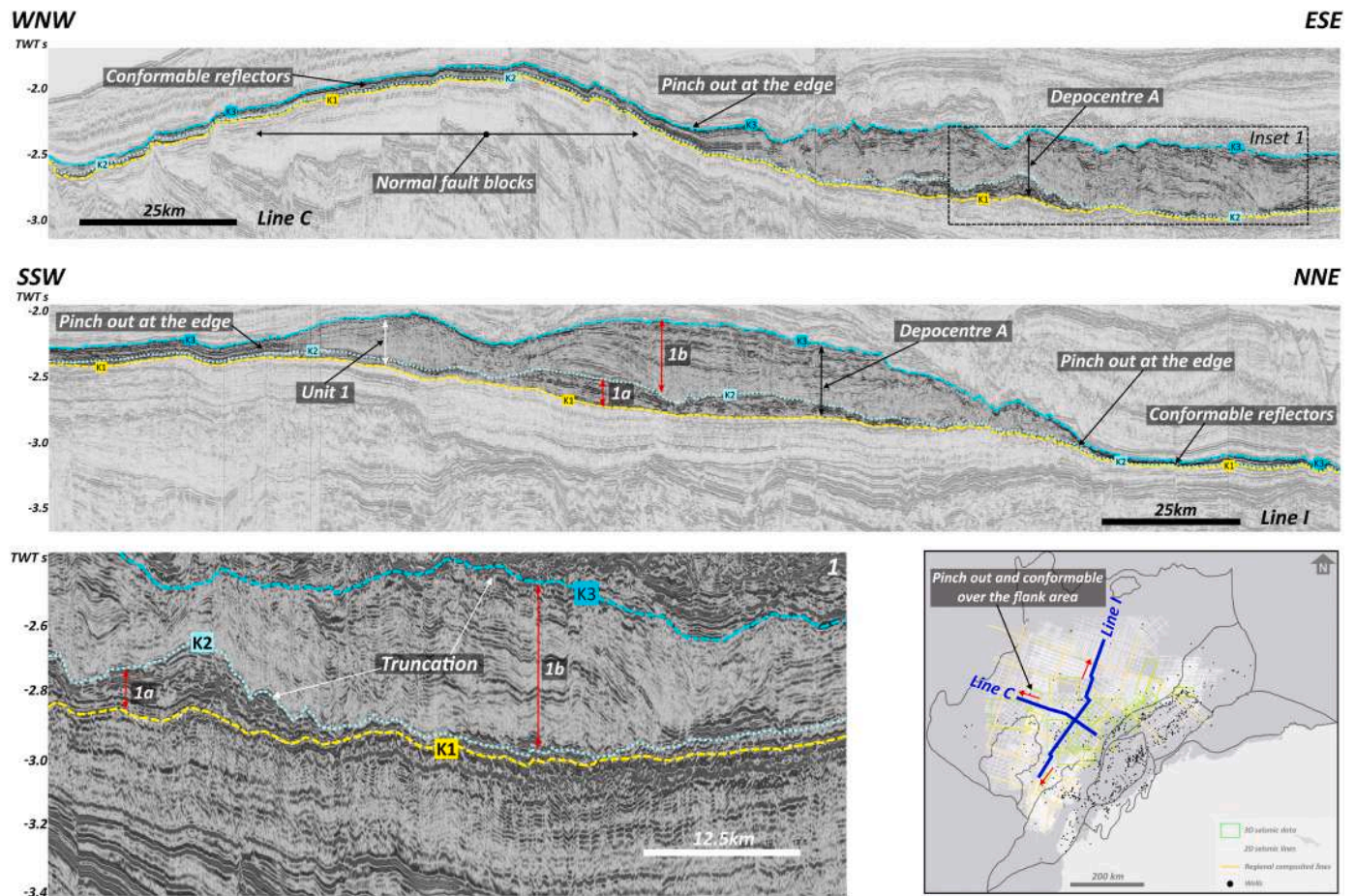


Fig. 9. Detail of regional seismic lines C and I displaying the nature of depocentre A. Sequences are thin and conformable on the flanks and at the edge of the depocentre. Prominent unconformities corresponding to horizons K1, K2 and K3 can be seen within the depocentre.

Australia (2015), but additional surfaces were also interpreted where significant changes in sedimentary style were observed.

The regionally correlatable seismic markers were used to define units based on the similarity of dominant seismic facies and hence do not always correspond to the play-based sequences of Marshall and Lang (2013). K0 represents the Valanginian Unconformity which marks the beginning of post-rift sedimentation and the development of a widespread transgressive unit that can be easily correlated over large parts of the NW Shelf resulting in the establishment of a widespread fully marine shelf (Barber, 1988; AGSO North West Shelf Study Group, 1996; Longley et al., 2002; Norvick, 2002; Marshall and Lang, 2013). The top of the Muderong Shale (Horizon K1) marks the onset of much more variable seismic facies. Consequently, the sequence above this is divided into four primary units which are Unit 1: Aptian – Turonian  $\approx$  K40.0 SB – K50.0 SB (Early to Late Cretaceous), Unit 2: Turonian – Rupelian  $\approx$  K50.0 SB – T30.0 SB (Late Cretaceous to Early Oligocene), Unit 3: Rupelian – Tortonian  $\approx$  T30.0 SB – T40.0 SB (Early Oligocene to late Miocene) and Unit 4: Tortonian – Present  $\approx$  T40.0 SB – Recent SB (late Miocene to Present) (Figs. 2–4).

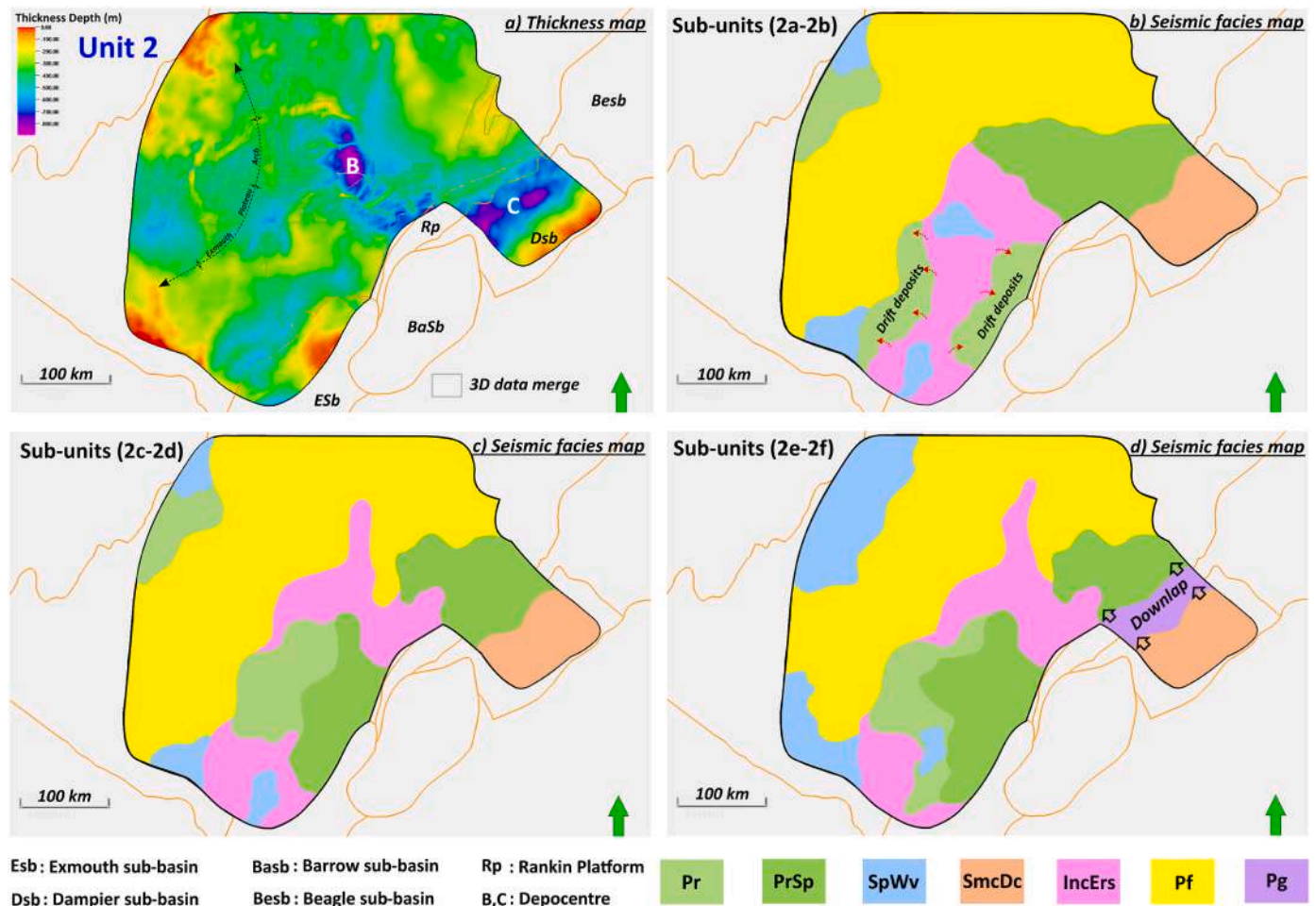
The main surfaces were depth converted using the average interval velocity of each unit compiled from checkshot and vertical seismic profile (VSP) data from 10 wells. The interval velocities used range from 1712.06 m/s for Unit 1 (the oldest unit), through 1639.99 m/s for Unit 2 and 1571.87 m/s for Unit 3–1515.80 m/s for Unit 4 (the youngest unit). The velocity of seawater is between 1490 and 1500 m/s. Isopach maps for each unit were derived from the maps of the main surfaces. Seismic facies maps of the primary units illustrate the distribution of different facies. The facies maps combined with well data (GR, cores, lithology, biostratigraphy and palynology) were used to determine depositional

environment. Together these are utilised to describe the post-Valanginian evolution of the passive margin.

#### 4. Regional seismic stratigraphic framework

The sequence between the Valanginian Unconformity and the base of Unit 2 mainly comprises fine-grained clastic sediments, while Units 2 to 4 are predominantly composed of fine-grained carbonates (Cathro, 2002; Moss et al., 2004; Chongzhi et al., 2013; and ditch cuttings from wells in the Exmouth Plateau), but also include siliciclastic sediments of early Paleocene and late Miocene age (Figs. 2–4 and 6).

K0 to K1 (Early post-rift) represents the Valanginian to Aptian stratigraphic interval, equivalent to K20.0SB to K40.0 SB (Figs. 2b and 3) of Marshall and Lang (2013). Over large parts of the Exmouth Plateau this interval is only a few metres thick (Fig. 7a), and thins and onlaps onto the remnant paleobathymetric expression of rotated fault blocks to the north and west (seismic line A and C on Fig. 4). Significant depocentres with up to 650 m of sediment are present in the Dampier sub-basin and in a bathymetric low in front of the Lower Barrow Shelf Edge (Fig. 7a). A more subtle depositional lobe associated with the Upper Barrow shelf is present on the NW margin of the Exmouth sub-basin. Over almost the entire area this interval is characterised by parallel to subparallel reflections (PrSp) and polygonal faults (Pf), with low angle progradational and aggradational clinofolds (Pg/Ag) present in the lower part of the sequence in the vicinity of Upper Barrow Shelf (Fig. 7b). Lithologically this interval corresponds to the Muderong Shale, with the lower parts laterally equivalent in the southeast to the Zeppard and Birdrong Formations of the Upper Barrow Group and to the Mardie Greensand Formation.



**Fig. 10.** Unit 2 comprises 6 sub-units, namely 2a-2f. a) Thickness map of Unit 2 with sediment depocentres B and C. This map was made from horizons T4 and K3. b, c, d) Seismic facies maps of Unit 2 express three dominant seismic characteristics: polygonal faulting, stacked incisions, and parallel and subparallel (see Table 2 for colour legend). Pr (Parallel), PrSp (Parallel to Subparallel), SpWv (Subparallel to Wavy), SmcDc (Semi-to discontinuous), IncErs (Incision or Erosive), Pf (Polygonal fault), Pg (Progradation).

#### 4.1. Unit 1 – horizons K1–K3 (~123.3 Ma Aptian – ~95 Ma Turonian)

Unit 1 conformably overlies the Muderong Shale. It is bounded at its base by horizon K1 (K40.0 SB of Marshall and Lang, 2013), and its top by horizon K3 (K50.0 SB of Marshall and Lang, 2013). It is divided into two sub-units (1a and 1 b) by horizon K2. It is less than 150 m thick over most of the Exmouth Plateau (Fig. 8a). A distinct sediment accumulation in the southeast of the NCB, centred over the Exmouth sub-basin, and running over the basin flank to the northwest, is up to 700 m in thickness (Fig. 8a).

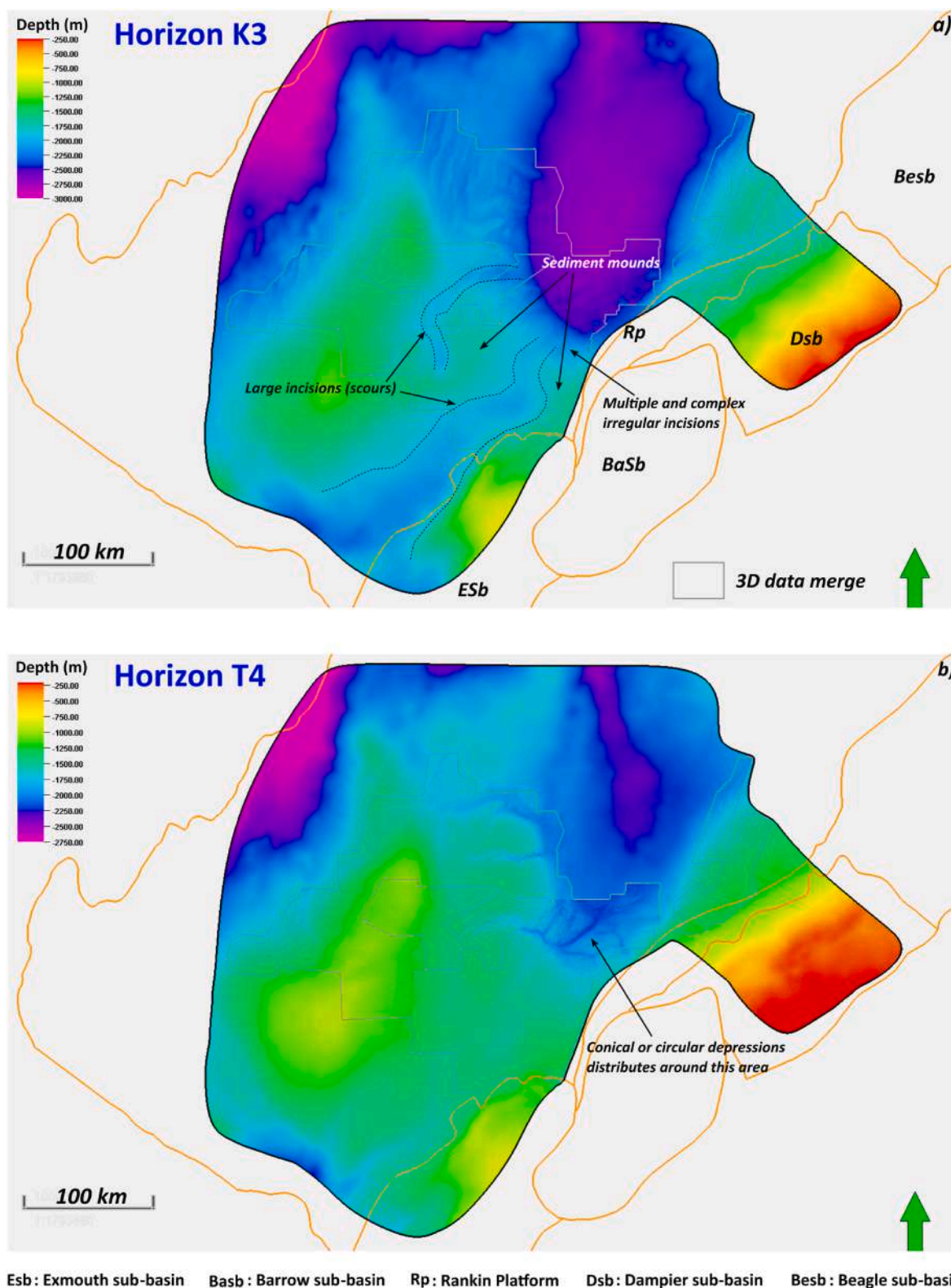
Horizon K1 is mostly a high amplitude, laterally continuous reflection that also locally onlaps onto rotated fault blocks in the northwest of the Exmouth Plateau (seismic line A and C on Fig. 4). Horizon K3 is a medium amplitude reflection that is generally conformable but forms a prominent unconformity in the southeast in the vicinity of the depocentre (Fig. 9). Horizon K2, which marks the boundary between sub-units 1a and 1 b, is a low amplitude, conformable reflection that onlaps and downlaps onto horizon K1 at the edge of the depocentre (Fig. 9).

The dominant seismic facies of Unit 1 within the depocentre is characterised by subparallel to wavy (SpWv), medium to high amplitude reflections (Fig. 8b), indicating the presence of subtle bedforms, which combined with the increased sediment thickness, may correspond to sediment mounds. Subparallel reflections mostly appear in sub-unit 1a (horizons K1–K2) and wavy reflections are more developed in sub-unit 1

b (horizons K2–K3). Away from the depocentre Unit 1 consists of parallel to subparallel (PrSp) seismic reflections (Fig. 8b), with a zone of parallel (Pr) reflections (Fig. 8b) in the southern part of the study area, showing more uniform deposition.

In wells, horizon K1 corresponds to the top of the Muderong Shale Formation (Figs. 5 and 6). K1 is the most laterally consistent reflector and is present over the whole basin. Deposition of the Muderong Shale terminated in the Aptian (AGSO North West Shelf Study Group, 1996; Longley et al., 2002; Norvick, 2002; well reports), and the top of this unit (K1) is also referred to as the Intra-Aptian Unconformity. However, for the most part it is conformable, apart from where it onlaps rotated fault blocks, or where there is a time gap generated by the onlap of sub-unit 1a.

Sub-unit 1a coincides with radiolarian-rich sediment in most wells (Figs. 3, 5 and 6), corresponding to the Windalia Radiolarite (Ellis, 1987; Bradshaw et al., 1988; Longley et al., 2002). This formation developed regionally until the latest Aptian or earliest Albian (Longley et al., 2002; Jablonski and Saitta, 2004). The top of this sub-unit corresponds to horizon K2. Horizon K3 is the top of sub-unit 1 b and ties to wells at the top of the Lower Gearle Siltstone and the Haycock Marl intervals (Figs. 3, 5 and 6). These formations were deposited during the Turonian. The Lower Gearle Siltstone generally consists of siltstones and shales but passes laterally into marls in the Haycock Marl (AGSO North West Shelf Study Group, 1996).



**Fig. 11.** Depth structure maps of horizons K3 and T4 showing examples of the erosional features associated with bottom current activity during the Turonian to Early Oligocene.

**4.2. Unit 2 – horizons K3-T4 (~95 Ma Turonian – ~30 Ma Rupelian)**

Unit 2 is separated from Unit 1 by horizon K3 at the base and is bound by horizon T4 (T30.0 SB of Marshall and Lang, 2013) at the top. It encompasses six seismic sequences and contains up to 550 m of sediment

over most of the NCB (Fig. 10a). Specific depocentres in the centre of the Exmouth Plateau, and at the northern margin of the Dampier sub-basin contain sediments up to 800 m in thickness (Fig. 10a) and may in part correspond to large scale sediment drifts (Fig. 11a).

The six seismic sequences in Unit 2 are bounded by horizons K4, K5,

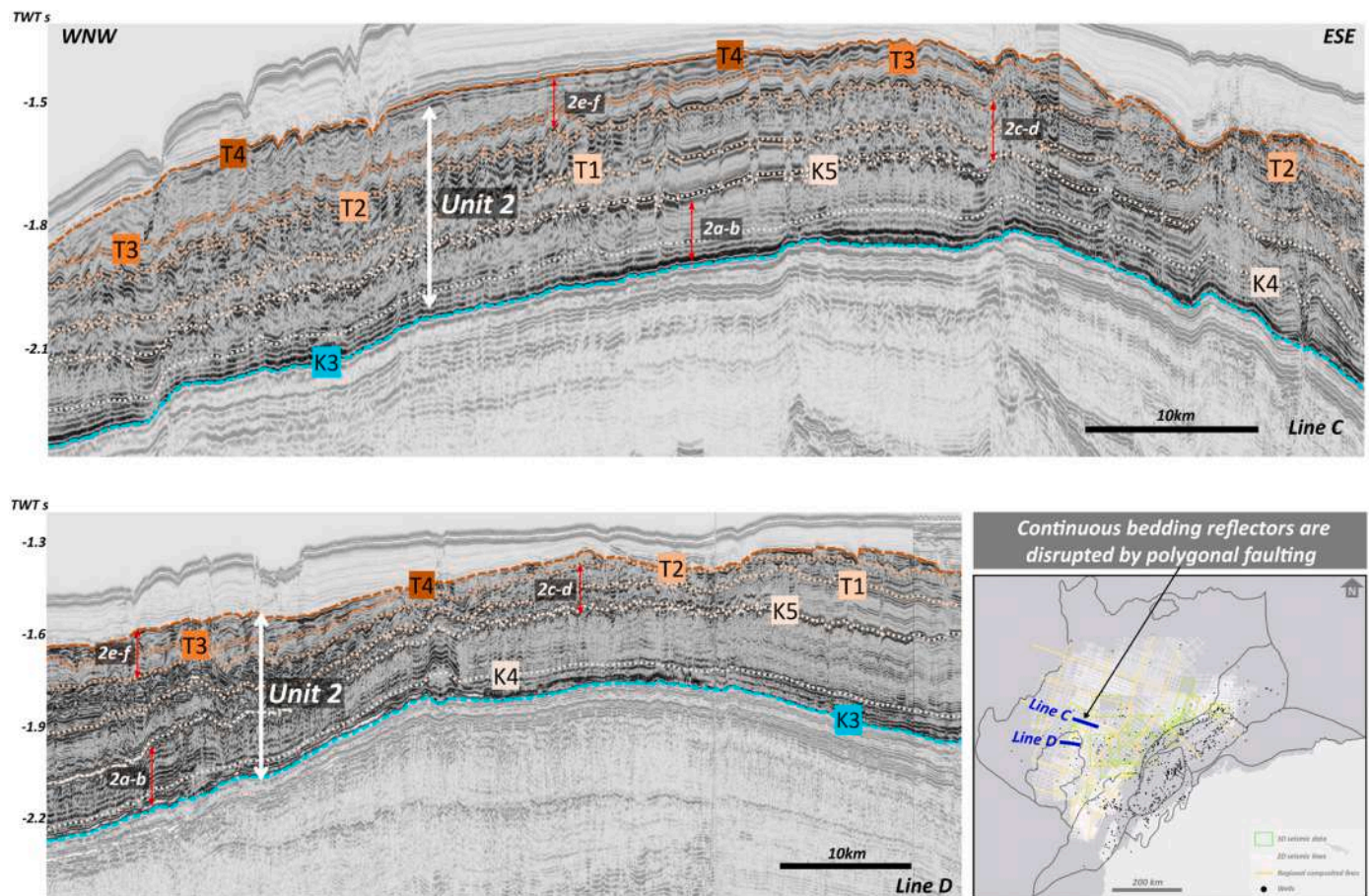


Fig. 12. Horizons K4, K5, T1, T2, T3 and T4 in Unit 2 (see seismic line C and D on the map) disrupted by polygonal faults, which are widespread across the most of the NCB. Location shown on the inset map.

T1 (K60.0 SB, T10.0 SB, T20.0 SB of Marshall and Lang, 2013, respectively), and by horizons T2, T3 and T4 (T30.0 SB). In general, the seismic horizons are characterised by relatively constant amplitude reflections in the northwest and northern area of the Exmouth Plateau and in the area surrounding the Investigator sub-basin (Fig. 1a), where they are correlated using consistent stratigraphic markers from wells. In these areas, the sequences are characterised by conformable, laterally continuous reflections of medium-high amplitude that are disrupted by a series of small offset faults (Fig. 12). In contrast, in the southeast of the area, near the Exmouth sub-basin and Rankin Platform, the equivalent surfaces are marked by complex stacked erosional truncations. The sequences within this area are also characterised by irregularly stacked incisions (Fig. 13). In addition, horizons T2, T3 and T4 represent downlap surfaces of low amplitude in the northeast - near the Dampier sub-basin (Fig. 14).

Unit 2 contains a great variety of seismic facies. The most common acoustic facies are the semi-continuous or parallel disrupted reflections with small offset faults, similar to those described as polygonal faults (Cartwright, 1994; Watterson et al., 2000). The polygonal faults (Pf) show a variation of styles with different degrees of rotation and disruption of the beds (Fig. 12). The faults are present in all six seismic sequences over a large part of the NCB but are mainly seen in the north and west (Fig. 10b, c, d). However, the polygonal faulted facies is less prominent in the older sequences in the south. Polygonal faults typically form in fine-grained sediments, indicating that this is the dominant lithology in these areas. The second most common acoustic facies is incised (IncErs) reflections (Fig. 10b, c, d, and Fig. 13). The reflections are characterised by simple incisions and complex stacked erosional truncations, which overlie and crosscut one another. The erosional

surfaces are associated with mounded reflections (Fig. 15), representing a composite of both erosional and depositional features, comparable to similar features described by Hernández-Molina et al. (2003; 2006) from the Gulf of Cadiz. The incised reflections are progressively replaced by parallel (Pr) and parallel to subparallel (PrSp) reflections, going up sequence from sub-units 2c to 2f (Fig. 10b, c, d). In addition, parallel and parallel to subparallel reflections also appear in the Dampier sub-basin, Rankin Platform, and in the northwest at the edge of the Exmouth Plateau. The parallel reflections change laterally into subparallel to wavy (SpWv) reflections in sub-units 2e and 2f (Fig. 10d). In the northeast of the Exmouth Plateau near the Dampier sub-basin, seismic reflectivity in sub-units 2e and 2f is expressed by downlapping reflections that show the initial growth of clinoforms which are more significantly developed in Units 3 and 4.

Horizon K4 at the top of sub-unit 2a is close to the top of the Upper Gearle Siltstone and the Toolonga Calcilitite in most available wells (Figs. 3, 5 and 6). These formations were deposited during the latter part of the Turonian and the Campanian. The lithology of the Upper Gearle Siltstone is similar to the Lower Gearle Siltstone, but it is more widespread and typically unconformably overlies the Lower Gearle Siltstone. In the northern part of the NCB, the Gearle Siltstone is generally thin, and it is replaced by the Toolonga Calcilitite. Lithologically, the Toolonga Calcilitite contains carbonate-rich sediments. The top of sub-unit 2 b at horizon K5 is assigned to the top of the Withnell Formation and the Miria Marl, which together developed during the latter part of the Campanian and the Maastrichtian (Figs. 3, 5 and 6). The Withnell Formation primarily consists of fine-grained limestones but corresponds to marls in the Miria Marl. The Miria Marl interval is thin, and sometimes it is not differentiated from the Withnell Formation. The top of sub-unit 2 b

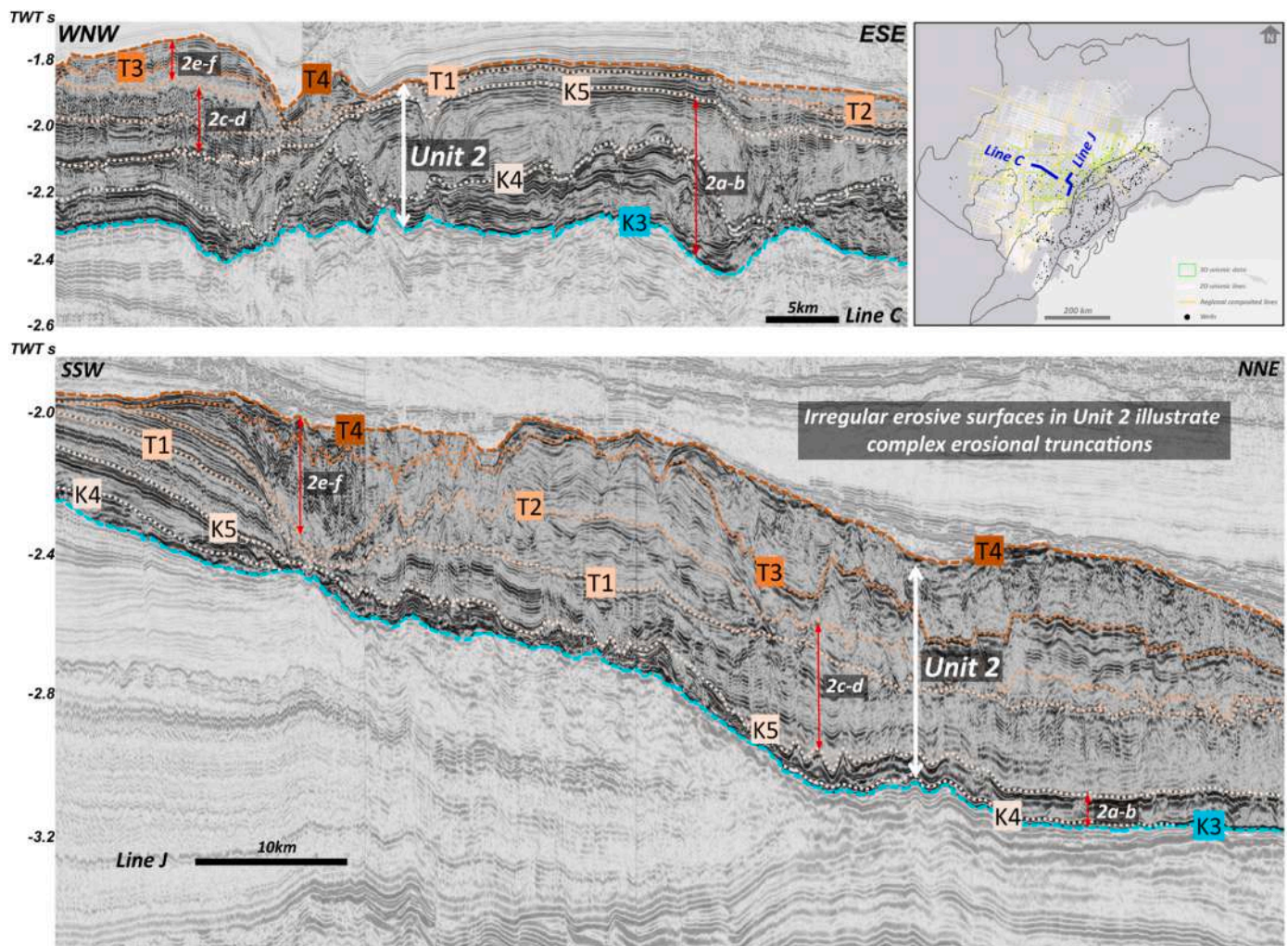


Fig. 13. Unconformable boundaries corresponding to Horizons K4, K5, T1, T2, T3 and T4, show multiple stacked incisions (location shown on the inset map).

(K5) is referred to as the Base Tertiary Unconformity.

In most wells, the top of sub-unit 2c (T1) corresponds to the top of the Lambert and Dockrell Formations, which developed in the Paleocene (Figs. 3, 5 and 6; AGSO North West Shelf Study Group, 1996; Cathro, 2002; Payenberg et al., 2013; Geoscience Australia, 2015; well reports). The Lambert Formation mainly contains claystone, but the Dockrell Formation is more marly (AGSO North West Shelf Study Group, 1996; Alrefae et al., 2018; Cathro, 2002; well reports). Meanwhile, the top of sub-unit 2 d at horizon T2 corresponds to the top of the Wilcox and Cardabia Formations that were deposited in the early and middle Eocene (Figs. 3, 5 and 6; AGSO North West Shelf Study Group, 1996; Cathro, 2002; Payenberg et al., 2013; Geoscience Australia, 2015; well reports). The Wilcox Formation consists of marls, and the Cardabia Formation contains relatively condensed fine-grained carbonates. Sub-units 2e (with its top at T3) and 2f (with its top at T4) are correlated to the Giralia Formation but in the northern and southwestern parts of the NCB they correspond to the laterally equivalent Lower Walcott Formation in sub-unit 2e which can be distinguished from the Upper Walcott Formation in sub-unit 2f. These formations were deposited in the middle Eocene and the early Oligocene. Lithologically, the Giralia Formation is similar to the Cardabia Formation, while the Walcott Formation consists of foraminiferal limestones and calcareous siltstone. The top of sub-unit 2f (T4) is referred to as the Oligocene Unconformity.

#### 4.3. Unit 3 – horizons T4-T6 (~30 Ma Rupelian – ~7 Ma Tortonian)

The third seismic stratigraphic unit downlaps onto horizon T4 at the top of Unit 2 and is bounded by horizon T6 (T40.0 SB of Marshall and Lang, 2013) at its top (Fig. 18a). It is subdivided by horizon T5 into two seismic sequences (sub-units 3a and 3 b). Overall, Unit 3 is less than 100 m thick, and it is mostly confined to the northeast of the NCB (Fig. 16a). A significant depocentre occurs in the northern part of the Dampier sub-basin and the Rankin Platform, containing sediments up to 550 m in thickness (Fig. 16a).

Horizons T5 and T6 are unconformable reflections of medium-high amplitude that form downlap surfaces. Seismic reflectivity in sub-unit 3a is characterised by steeply downlapping simple sigmoid reflections (Fig. 18a), while sub-unit 3b presents more complex sigmoid geometries with gentle to high angle downlapping reflections (Fig. 18a). In general, the clinofolds in Unit 3 show strongly progradational (Pg) stacking patterns (Fig. 18a) and appear primarily in the area of the Rankin Platform and the Dampier sub-basin (Fig. 16b). This acoustic facies passes laterally into subparallel (PrSp) reflections in more distal areas (Fig. 16b), and then into semi-chaotic (SmCh) reflections that downlap onto horizon T4 (Fig. 16b). These seismic characteristics are evidence of submarine mass failure events.

In most wells, sub-unit 3a correlates to the Mandu Formation of late Oligocene and early Miocene age (Figs. 3, 5 and 6). This deposit consists of both coarse and fine-grained carbonate sediment including some reef facies (Tortopoglu, 2015; Alrefae et al., 2018). Sub-unit 3b corresponds

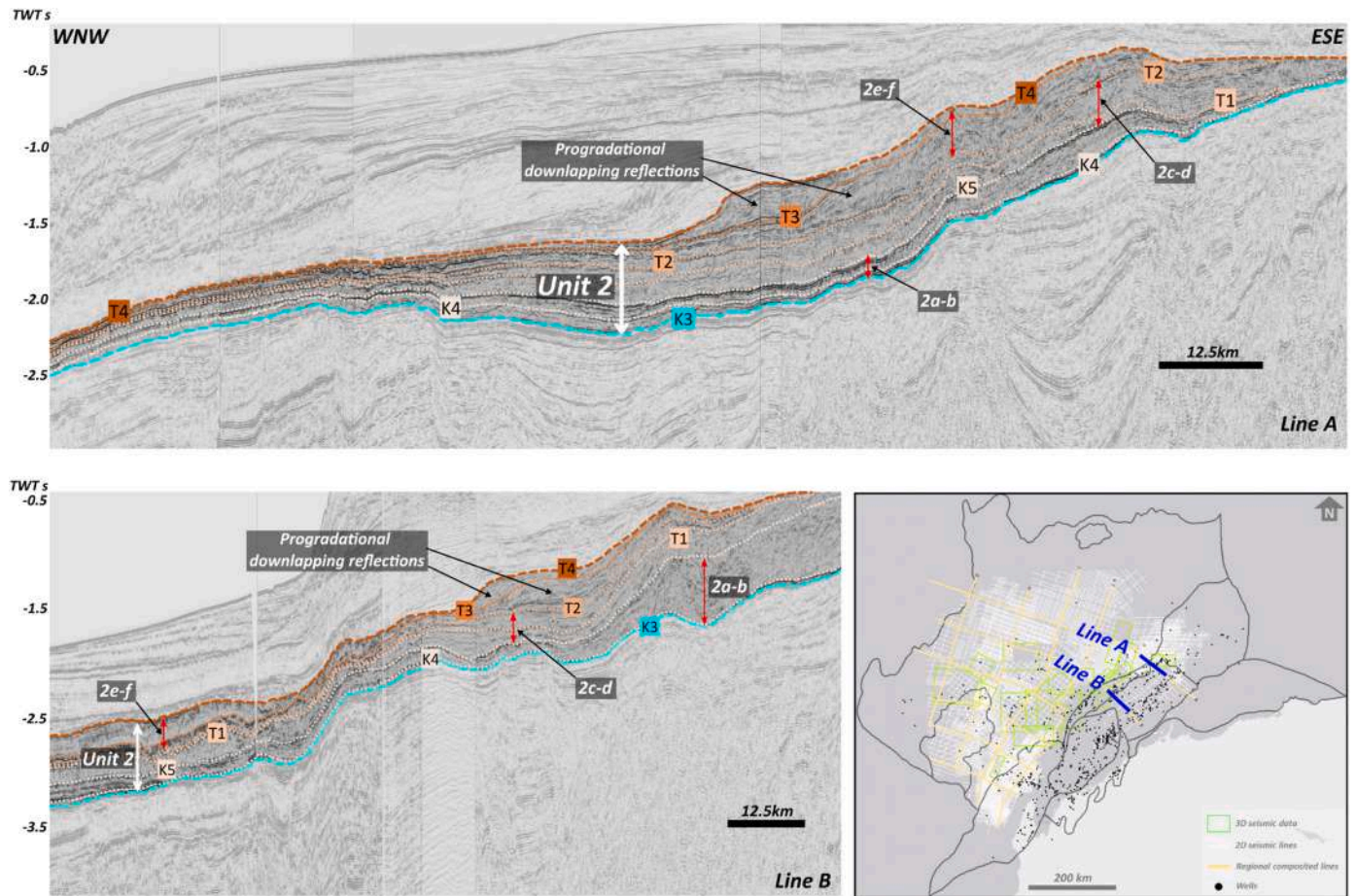


Fig. 14. Horizons T2, T3 and T4 in the northeast area close to the Rankin Platform and the Dampier Sub-basin are major downlap surfaces (location shown on the inset map).

to the Trealla and Bare Formations, which were deposited during the Middle and Late Miocene (Figs. 3, 5 and 6). The uppermost part of the Trealla Limestone passes laterally into sands of the Bare Formation.

#### 4.4. Unit 4 – horizons T6-T10 (~7 Ma Tortonian – 0 Ma present)

Unit 4 is the youngest seismic stratigraphic unit and it unconformably overlies horizon T6 of Unit 3 in the northeast and horizon T4 of Unit 2 in the remainder of the NCB. Its top is horizon T10 (seabed). Unit 4 comprises four seismic sequences, which contain sediment up to 350 m thick over most of the area (Fig. 17a). A distinct depocentre in the northeast part of the Rankin Platform has more than 650 m of sediment (Fig. 17a).

Horizons T7, T8, T9 are unconformable reflections of medium-high amplitude, expressed by downlap surfaces in the northeast (Fig. 18b). Here, the surfaces separate four sub-units (4a-4d) characterised by downlapping reflections (Pg in Fig. 17b and c) with complex sigmoidal geometries. In contrast, in the northern and southern part of the area all the horizons are semi-continuous and continuous reflections of low-medium amplitude (Fig. 18b), and the main acoustic facies of all the sub-units comprise chaotic reflections (Ch: Chaotic, SmCh: Semi Chaotic and PrCh: Parallel to Chaotic in Fig. 17b and c), parallel (Pr) and parallel to subparallel (PrSp) reflections (Fig. 17b and c). The clinoforms in Unit 4 are mainly progradational and slightly aggradational. In the shelf break areas, the clinoforms are overlain and crosscut by gullies or channels on slopes (Fig. 19). The chaotic acoustic facies is more widespread in sub-units 4a to 4c (Ch: Chaotic, SmCh: Semi Chaotic and PrCh: Parallel to Chaotic in Fig. 17b) and much less extensive in sub-unit 4d (Fig. 17c). This wide distribution of chaotic facies shows multiple mass

failure events that happened at the time of deposition. Besides, sub-unit 4d is characterised by parallel (Pr) and parallel to subparallel (PrSp) reflections (Fig. 17b and c). However, on the northwest at the edge of the Exmouth Plateau, it is expressed by subparallel to wavy (SpWv) reflections that developed from sub-units 4a to 4d (Fig. 17b and c).

Unit 4 corresponds to the Delambre Formation in most available wells (Figs. 3, 5 and 6). This formation was deposited during the late Miocene to Recent. Lithologically, the Delambre Formation is similar to the Mandu Formation (Tellez, 2015; Alrefaee et al., 2018).

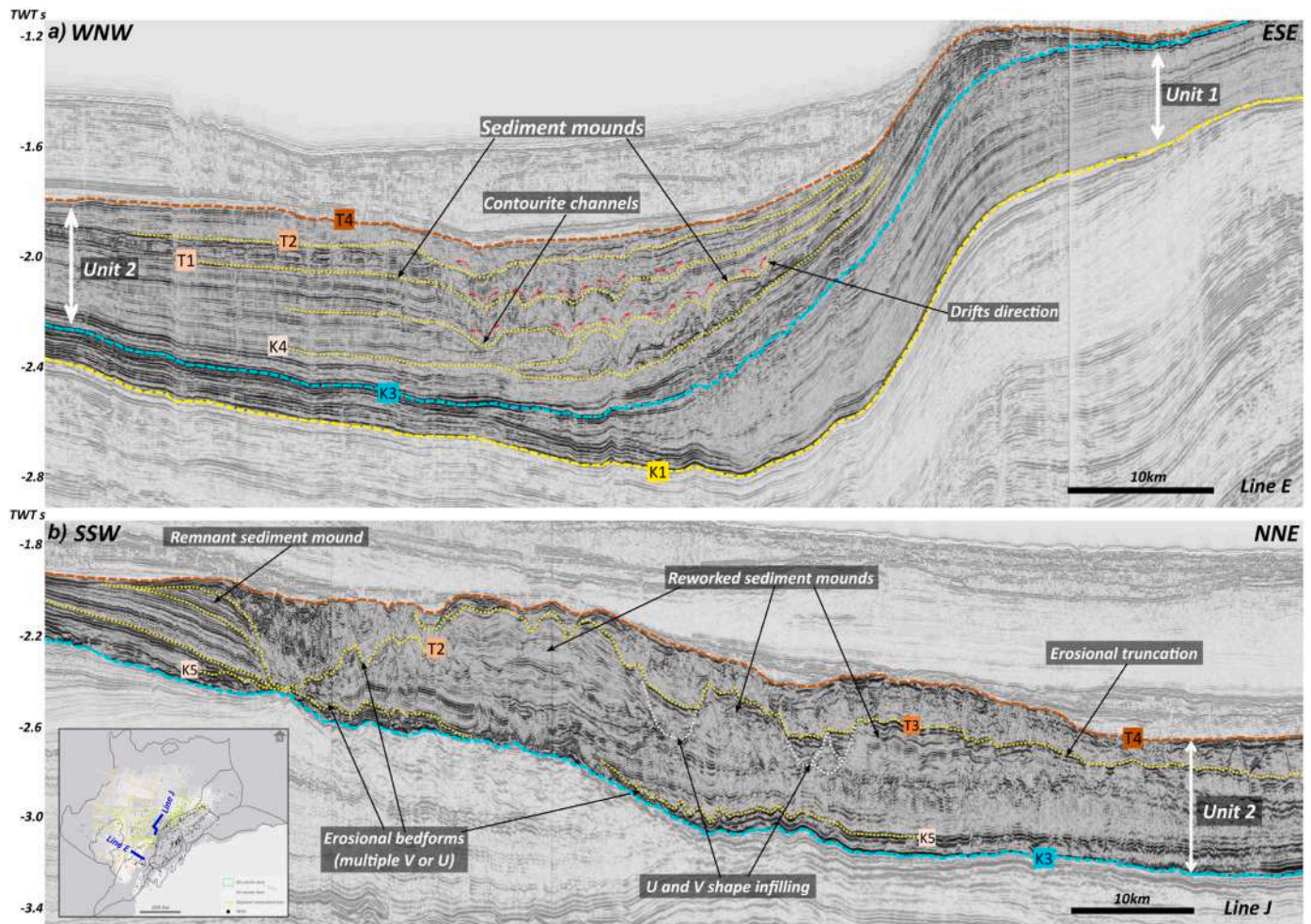
## 5. Evolution of the post-valanginian sequence in the NCB

From the integration of seismic and well data, we are able to demonstrate four distinct phases in the post-rift evolution of the Northern Carnarvon Basin: an initial phase of subsidence from the Valanginian to the Turonian, a period from the Turonian to the Early Oligocene dominated by bottom current activity in parts of the basin, the establishment of prograding carbonate shelves in the Late Oligocene to Late Miocene and the widespread development of mass transport complexes from the Late Miocene to Present.

### 5.1. Valanginian to Turonian: post breakup subsidence

During the Berriasian, prior to breakup, the NCB was characterised by the Lower Barrow Group which comprises a clastic shelf located in the south east portion of the basin, turbidite fans fed by southerly derived turbidity currents and laterally equivalent distal muds which accumulated in deeper water settings to the northwest (Paumard et al., 2018).





**Fig. 15.** The evidence for bottom currents in Unit 2. a) In seismic line E, the currents caused sediment drifts and created sediment mounds. b) In seismic line J, the currents were more energetic, creating highly eroded beds and simple to complex scours (location shown on the inset map).

As a consequence of Valanginian breakup, sediment supply from the south was terminated marking the end of deposition of the Lower Barrow Group. However, uplift and erosion in the Exmouth sub-basin resulted in the deposition of a separate deltaic sequence referred to as the Upper Barrow Group (Arditto, 1993). This is succeeded in the Hauterivian by the glauconitic Mardie Greensand Member which represents a significant phase of transgression as relative sea level began to rise on the subsiding continental margin (Geoscience Australia, 2015). The transgression continued during the Aptian, resulting in the deposition of the Muderong Shale (AGSO North West Shelf Study Group, 1996; Longley et al., 2002; Norvick, 2002; Marshall and Lang, 2013), which is clearly imaged on seismic sections, showing generally continuous reflections with high to medium amplitudes. Further marine transgression continued through the deposition of Unit 1 in the Aptian – Turonian, where deposition of the *Wendalia Radiolarite* occurred during the Aptian (Bradshaw et al., 1988). This unit resulted in widespread deposition of fine-grained sediment represented by parallel and subparallel seismic facies. However, the development of mounded features characterised by wavy seismic facies in the southeast part of the basin suggests the initiation of bottom current activity and the development of large scale mounds in this part of the shelf (Stow et al., 2009; Rebesco et al., 2014).

## 5.2. Turonian to Early Oligocene: bottom current activity

Horizon K3 (or K50.0 SB) marks a significant change in the style of deposition, characterised by stacked incisions and sediment mounds

which are laterally equivalent to more uniform beds (polygonally faulted sequences) elsewhere in the basin. The complex stacked incision seismic facies is likely evidence of energetic bottom currents while the polygonally faulted sequences generally form in fine-grained sediments (Cartwright et al., 2003) and represent a continuation of a low energy environment. This bimodal distribution of facies continues through the whole of the Turonian – Rupelian stratigraphic interval represented by Unit 2.

Ocean bottom currents promote the formation of erosional surfaces as well as depositional features, such sediment drifts and bedforms, with different geometries and dimensions (Stow et al., 2002; Rebesco et al., 2014; Ercilla et al., 2016) depending on the velocity of the currents and the availability of sediments (Masson et al., 2004; Hernández-Molina et al., 2006; Stow et al., 2009). During the Late Cretaceous (sub-unit 2 ab), large scours and sediment mounds as well as numerous smaller irregular scours were developed in the southeast of the Exmouth Plateau near the Rankin Platform and Exmouth sub-basin (Figs. 10b, 11a and 13). The largest depressions are visible on the basal surface of Unit 2 (horizon K3, Fig. 11a) and dissect the large-scale mounds developed towards the top of Unit 1. The largest depression is 221 km long and up to 67 km wide. The base of these depressions are partially erosional, and partially depositional (Fig. 11a) implying that the currents redistributed and transported fine-grained sediments on either side of the depression to form smaller scale sediment mounds (Rebesco and Stow, 2001; Stow et al., 2002; Rebesco, 2005; Hernández-Molina et al., 2008).

These depressions are filled by multiple stacked sediment bodies

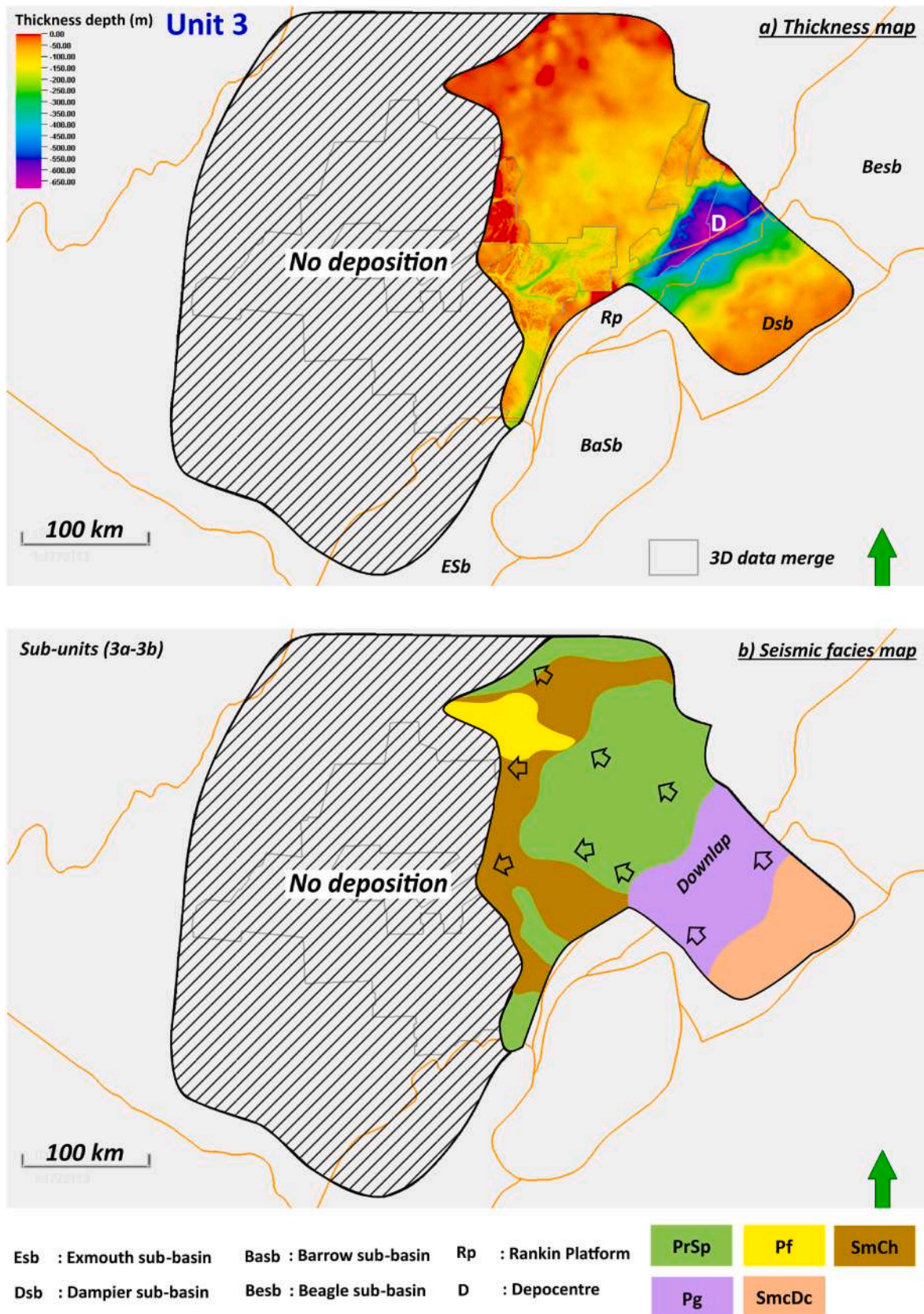
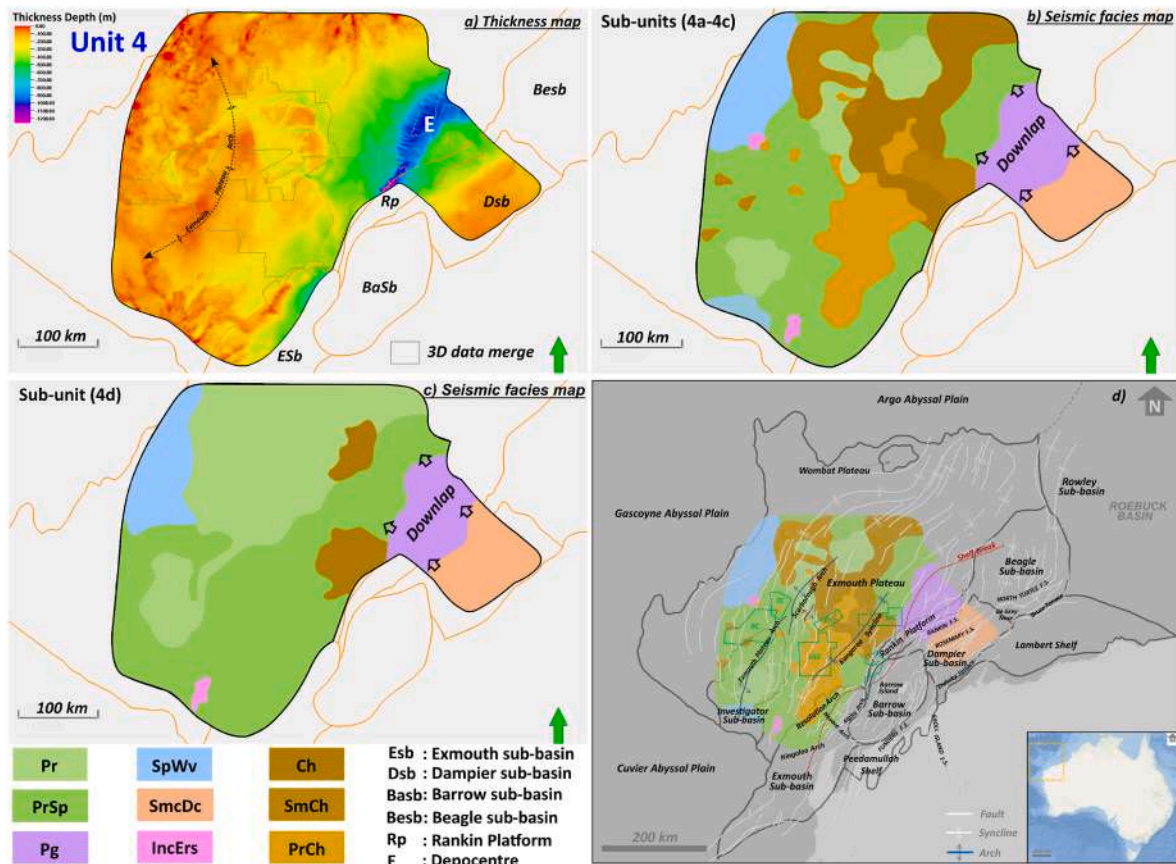


Fig. 16. a) Thickness map of Unit 3 with sediment depocentre D. This map was derived from horizons T6 and T5. b) Seismic facies maps of Unit 3, which contains sub-units 3a and 3 b (see Table 2 for colour legend). PrSp (Parallel to Subparallel), Pf (Polygonal fault), SmCh (Semi Chaotic), Pg (Progradation), SmcDc (Semi-to discontinuous).



**Fig. 17.** a) Thickness map of Unit 4 with sediment depocentre E. This map was generated from horizon T10 and the merger of horizons T6 of Unit 3 and T4 of Unit 2. b) Seismic facies map in sub-unit 4a-c shows widespread chaotic sediment. c) Sub-unit 4 d is mainly characterised by parallel and subparallel beds (see Table 2 for colour legend). d) MTCs distribution in the NCB. The green shapes show slope failure studies from Hengesh et al. (2012) in Gorgon (GC), Willem (WC), Glencoe (GLC) and Chadon Complexes (CC), and from Scarselli et al. (2013) in Thebe (TC) and Bonaventure Complexes (BC). Pr (Parallel), PrSp (Parallel to Subparallel), Pg (Progradation), SpWv (Subparallel to Wavy), SmcDc (Semi-to discontinuous), IncErs (Incision or Erosive), Ch (Chaotic), SmCh (Semi Chaotic), PrCh (Parallel to Chaotic).

which are characterised by parallel and subparallel beds (Fig. 10b, c, d, and Fig. 15a). They are also cut by multiple irregular scours which become increasingly common in the younger sequences and further down slope towards the north-east. The scours comprise multiple and cross cutting V and/or U-shaped incisions typically 2.5 km in width and 25 km in length, the largest of which are up to 6.5 km in width (horizons K4–K5, Fig. 15). We interpret these as sediment waves and contourite channels, indicating the presence of energetic bottom currents. These structures have also been recognised and similarly interpreted by Nugraha et al. (2019).

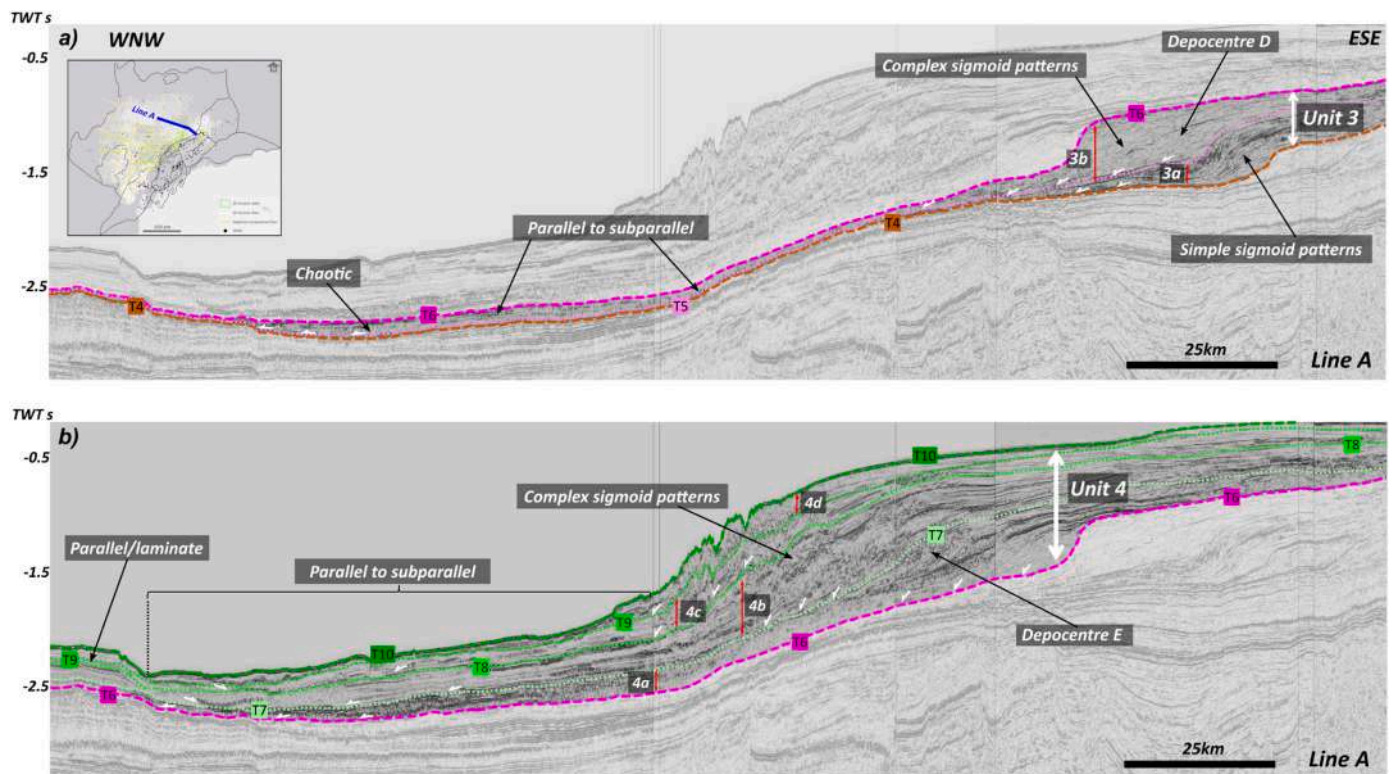
Erosive currents persisted into the Paleogene, particularly in the north of the area near the Rankin Platform. In addition, circular features are also visible on the base Paleogene surface (horizon T3, Fig. 15b and horizon T4 Fig. 11b) in the areas covered by 3D data. In cross section, the features are similar to the elongate V-shaped incisions described above (Fig. 15b), but are conical in shape and are similar to those described by Imbert and Ho (2012). These structures are common in part of the Exmouth Plateau near the Rankin Platform, and they are variable in size. The largest are 5 km in diameter and are filled by chaotic sediment packages. They lack the sediment drifts associated with erosive incisions and we interpret these features either as large pockmarks caused by fluid escape or the result of deep water carbonate dissolution.

The erosive current activity is much more pronounced in the southeast of the Exmouth Plateau near the Rankin Platform and represents significantly different conditions to those in the remainder of the Exmouth Plateau where uniform polygonal faulted sediments were deposited. The reason for this is unclear, but one possible explanation

might relate to the development of currents associated with the increasing separation of India from Australia. The onset of high energy current activity occurs in the Turonian, following a dramatic increase in the north-westward drift of India that began in the Albian (Veevers, 2000). This potentially enlarged oceanic circulation along the north-western margin of Australia, creating the potential for significant current activity on the NWS. Changes in relative sea level may also have influenced sedimentary processes but increases in the rate of tectonic subsidence in the Late Cretaceous (around 95 Ma and 65 Ma; Müller et al., 1998) and in the Paleogene (AGSO North West Shelf Study Group, 1996) are not coincident with any of the changes in sedimentary processes observed on the NWS. Similarly, there is no clear evidence that the Oligocene dissolution features formed at a time when there was a global sea level fall (Miller et al., 1991; AGSO North West Shelf Study Group, 1996).

### 5.3. Late Oligocene to Late Miocene: carbonate shelf

Another significant change occurs at horizon T4 (or T30.0 SB), which marks the cessation of bottom current activity and the onset of clinoform sequences during the Oligocene and Miocene, the dominant seismic facies of Unit 3. Full separation between Australia and Antarctica along the southeastern margin developed at this time (Gibbons et al., 2015) and may have further modified circulation with the development of new currents around the Southern Ocean. The clinoforms are mainly progradational and are consistent with the deposition of carbonates during subsidence which occurred during the Rupelian – Tortonian interval



**Fig. 18.** a, b). Seismic line A describes seismic facies Units 3 and 4. In the ESE, sub-unit 3a-3b and 4a-4d are illustrated by progradational patterns that form a simple sigmoid to complex patterns. Further WNW, seismic facies changes into parallel to subparallel and semi-chaotic facies, and it onlaps and terminates onto Horizon T4 and T6 (location shown on the inset map). The white arrows indicate downlapping and onlapping reflections.

(AGSO North West Shelf Study Group, 1996; Longley et al., 2002; Marshall and Lang, 2013). In addition, slope instability associated with more steeply dipping clinoforms resulted in slumps or mass-transport complexes (MTCs) in more distal areas. These features are clearly seen on seismic data, illustrated by semi-chaotic seismic facies within Unit 3 (Figs. 16b and 18a). However, the limited extent of Unit 3 is probably associated with the limited extent of shelf deposition, causing the sediments to downlap and onlap onto the top of Unit 2.

#### 5.4. Late Miocene to present: Mass transport complexes

The development of clinoforms, slumps and MTCs is much more widespread in Unit 4, starting from the late Miocene horizon T6 (or T40.0 SB) and particularly well developed in sub-units 4a-4c. Like Unit 3, clinoforms mainly occur in the northeast of the Rankin Platform, are mostly progradational and slightly aggradational.

Slope failures in the Exmouth Plateau are particularly common and are found in areas around the Kangaroo Syncline, the Resolution Arch and the Exmouth Plateau Arch (Fig. 17a, d). Hengesh et al. (2012) and Scarselli et al. (2013, 2020) studied the sediment collapses within the Neogene – Recent section on the SE and NW flanks of the Exmouth Plateau Arch e.g., the Glencoe and Chadon complexes of Hengesh et al. (2012), and the Thebe and Bonaventure complexes of Scarselli et al. (2013), as well as along the shelf break on the inboard margin of the Exmouth Plateau (e.g. Willem and Gorgon complexes, Fig. 17d). Slope failures in the Exmouth Plateau occurred in water depths ranging from 200 to 300 m at the shelf edge and adjacent to the deeper water parts of the NCB in water depths of more than 1500 m (Hengesh et al., 2012).

MTCs are associated with slope instability associated with the development of large clinoforms at the shelf slope break, and by increasing slope gradients in areas around the Resolution and Exmouth Plateau arches as a result of Miocene to Recent compression (Hengesh et al., 2012; Scarselli et al., 2013). The Exmouth Plateau Arch only

becomes visible on sediment thickness maps in Unit 4 (Figs. 7, 8 and 17) suggesting that it only developed from the Late Miocene onwards. Earthquake activity and increased slope angles caused instability in poorly consolidated sediments (i.e., fine-grained sediment of the Delambre Formation), while increased lateral loads and decreased stability develop in the shelf break and upper slope domain (Hengesh et al., 2012; Scarselli et al., 2013), as evidenced in other margin settings (Maselli et al., 2020). As a result, multiple stacked MTCs were generated with different sizes ranging in extent from ~20 to ~60 km. In the northern area on seismic line A (Fig. 19a), slumps and MTCs are mainly produced by sediment collapse from a topographic high near the NE flank of the Exmouth Plateau Arch. In addition, on seismic line B (Fig. 19b) the transported deposits are derived from the steep shelf slope breaks and extensive clinoforms in the east. On the southern side of the Exmouth Plateau, the shelf edge is above the Resolution Arch. Here, the slope gradient is gentle with much less volume represented by clinoforms. Submarine failures are also present, but the MTCs form single or double stacks less than 20 km in extent.

## 6. Summary and conclusions

This paper presents a regional seismic stratigraphic framework for the Northern Carnarvon Basin that highlights the evolution of sedimentary processes on the continental margin following Valanginian breakup. Detailed observations of the seismic characteristics of ten regional seismic sections that are tied to wells have been used to define the major seismic stratigraphic units. The units are defined by regionally correlatable boundaries, and are associated with distinct sedimentary facies and depositional sequences.

The four main stratigraphic units contain heterogeneous and complex sequences separated by multiple unconformities. Following widespread transgression from the Valanginian to the Aptian, the Aptian – Turonian succession of Unit 1 is generally thin with parallel bedding in

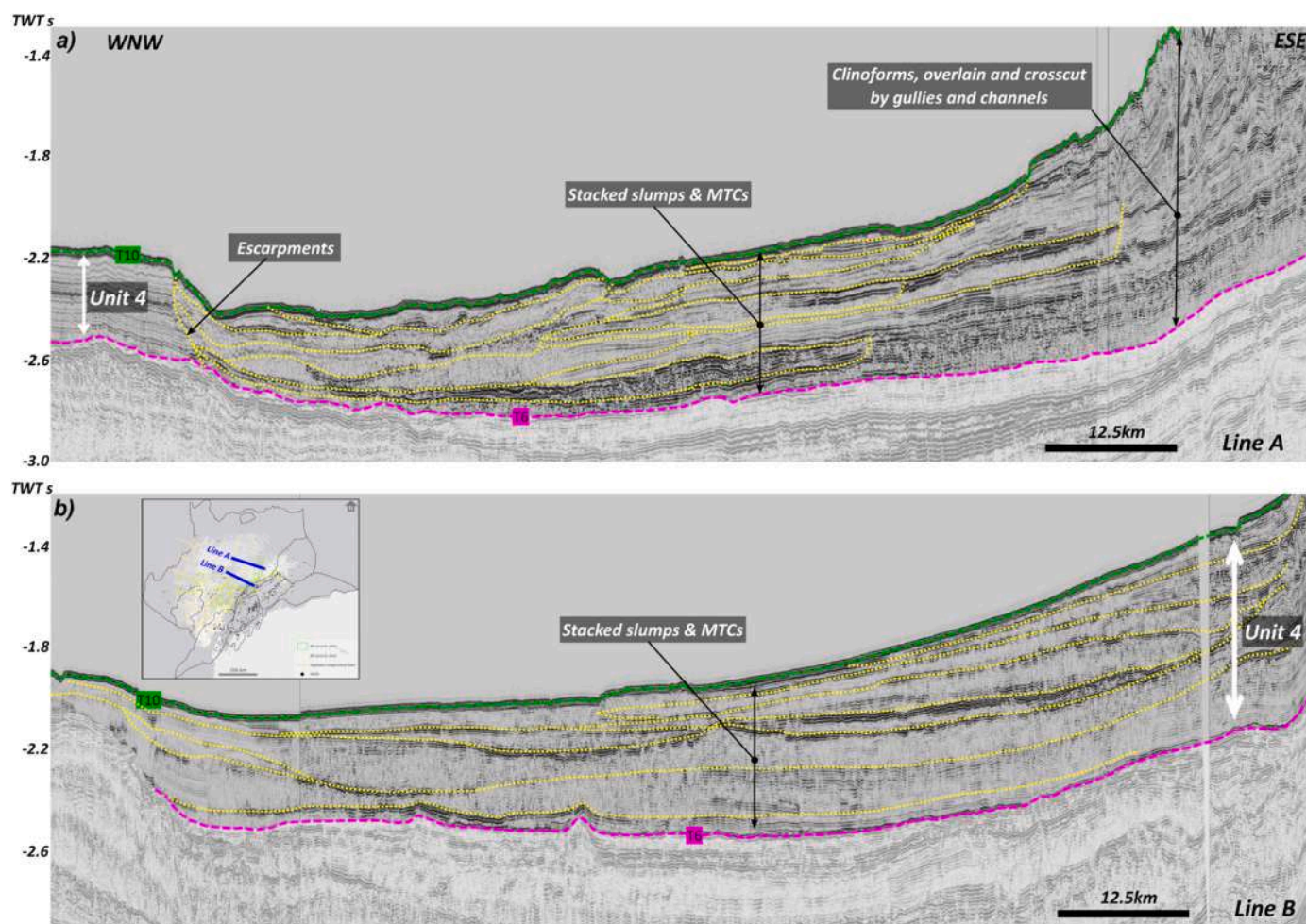


Fig. 19. a, b). Seismic lines A and B highlight slumps and MTCs in Unit 4 in the NW side of the Rankin Platform. In the line A, sediment collapses mainly from a topographic high in the west, which created escarpments and sediment runoff to the east. In line B, the slope gradient is steeper and was greatly affected by slope failure (location shown on the inset map).

the northwest of the Exmouth Plateau. The beds represent a uniform depositional environment. In the southeast, subparallel and wavy beds imply an increased influence of submarine currents and the initial development of sediment mounds in an outer shelf setting. In the Turonian – Rupelian succession of Unit 2, polygonal faulting occurring mainly in the north and west of the Exmouth Plateau shows a continuation of low energy depositional processes. Conversely, the southeast of the study area is dominated by multiple stacked incisions and sediment drifts, more widespread and varied than previously recognised, which indicate the presence of more active bottom currents. In the younger sequences, incisions are replaced by parallel and subparallel beds indicative of decreasing current energy. The Rupelian – Tortonian succession of Unit 3 marks the development of progradational clinoforms. The clinoforms formed at the shelf edge were subject to slope instability resulting in chaotic deposits. Sedimentary units terminate, onlap and downlap onto Unit 2. Chaotic sedimentary units are more extensively developed in the Tortonian – Recent succession of Unit 4. In addition to slope instability, the widespread distribution of chaotic sediments is also associated with the evolution of the Exmouth Plateau Arch and related seismic activity, and the accumulation of fine-grained sediments.

In conclusion, the interpretation of seismic reflection data in combination with well data reveals the complex stratigraphic evolution of the post-rift margin sequences in the Northern Carnarvon Basin. The variation in seismic facies is primarily controlled by the establishment of energetic bottom currents, from the Turonian to the Early Oligocene, and the emplacement of MTCs, since the Late Miocene, testifying to the

dynamic interaction of oceanographic and tectonic processes during the infill of the NCB. This study illustrates the complexity of the depositional and erosional processes that operate on a passive continental margin and demonstrates the need for further study to unravel the complex interplay of processes that give rise to such deposits in the basin.

#### Declaration of competing interest

The authors declare that they have no known competing financial interests or personal relationships that could have appeared to influence the work reported in this paper.

#### Data availability

Data will be made available on request.

#### Acknowledgements

We would like to express our gratitude to Geoscience Australia for the provision of public domain seismic and well log data. All available datasets used in this research are open source, can be accessed through the National Offshore Petroleum Information Management System (NOPIMS; <https://nopims.dmp.wa.gov.au/nopims>). Schlumberger are thanked for the provision of Petrel software. Mulky Winata is supported by a collaborative PhD scholarship under the Aberdeen – Curtin Alliance (<http://aberdeencurtinalliance.org/>) namely between Curtin University

(Perth, Australia) and the University of Aberdeen (Aberdeen, Scotland). Diego Kietzmann, Victorian Paumard, Marina Rabineau and two anonymous referees are thanked for their thoughtful reviews of earlier versions of this manuscript.

## References

- AGSO North West Shelf Study Group, 1996. Carnarvon cretaceous – tertiary tie report. In: Romine, K.K., Durrant, J.M. (Eds.), Australian Geological Survey Organisation.
- Apthorpe, M., 1988. Cainozoic depositional history of the North West Shelf. In: Purcell, P.G., Purcell, R.R. (Eds.), *The North West Shelf, Australia. Proceedings of the Petroleum Exploration Society of Australia Symposium*, Perth, WA, pp. 55–84.
- Alrefaee, H., Ghosh, S., Abdel-Fattah, M., 2018. 3D seismic characterization of the polygonal fault systems and its impact on fluid flow migration: an example from the Northern Carnarvon Basin, Australia. *J. Petrol. Sci. Eng.* 167, 120–130. <https://doi.org/10.1016/j.petrol.2018.04.009>.
- Arditto, P.A., 1993. Depositional sequence model for the post-barrow Group neocomian succession, Barrow and Exmouth sub-basins, western Australia. *APEA J.* 33, 151–160.
- Audley-Charles, M.G., Ballantyne, P.D., Hall, R., 1988. Mesozoic-Cenozoic rift-drift sequence of Asian fragments from Gondwanaland. *Tectonophysics* 155, 317–330. [https://doi.org/10.1016/0040-1951\(88\)90272-7](https://doi.org/10.1016/0040-1951(88)90272-7).
- Barber, P.M., 1988. The Exmouth Plateau deep water frontier: a case history. In: Purcell, P.G., Purcell, R.R. (Eds.), *The North West Shelf, Australia. Proceedings of Petroleum Exploration Society Australia Symposium*. Perth: WA, pp. 173–187.
- Borel, G.D., Stampfli, G.M., 2002. Geohistory of the North West Shelf: a tool to assess the palaeozoic and mesozoic motion of the Australian plate. In: Keep, M., Moss, S.J. (Eds.), *The Sedimentary Basins of Western Australia 3. Proceedings of the Petroleum Exploration Society of Australia Symposium*, pp. 119–128.
- Bradshaw, M.T., Yeates, A.N., Beynon, R.M., Brakel, A.T., Langford, R.P., Totterdell, J. M., Yeung, M., 1988. Palaeogeographic evolution of the North West Shelf region. In: Purcell, P.G., Purcell, R.R. (Eds.), *The North West Shelf, Australia. Proceedings of the Petroleum Exploration Society of Australia Symposium*, pp. 29–54.
- Bradshaw, J., Sayers, J., Bradshaw, M., Kneale, R., Ford, C., Spencer, L., Lisk, M., 1998. Palaeogeography and its impact on the petroleum systems of the North West Shelf, Australia. In: Purcell, P.G., Purcell, R.R. (Eds.), *The Sedimentary Basins of Western Australia 2. Proceedings of the Petroleum Exploration Society of Australia Symposium*, pp. 95–121.
- Butcher, B.P., 1989. Northwest shelf of Australia. In: Edwards, J.D., Santogrossi, P.A. (Eds.), *Divergent/Passive Margin Basins. AAPG Memoir*, 48, pp. 81–115. <https://doi.org/10.1306/M48508C2>.
- Cathro, D.L., 2002. Three-Dimensional Stratigraphic Development of a Carbonate-Siliciclastic Sedimentary Regime, Northern Carnarvon Basin, Northwest Australia. PhD Dissertation. The University of Texas at Austin, Austin, Texas, p. 490.
- Cathro, D.L., Austin Jr., J.A., Moss, G.D., 2003. Progradation along a deeply submerged Oligocene-Miocene Heterozoan carbonate shelf; how sensitive are clinoforms to sea level variations? *AAPG Bull.* 87, 1547–1574. <https://doi.org/10.1306/05210300177>.
- Cathro, D.L., Karner, G.D., 2006. Cretaceous–tertiary inversion history of the Dampier Sub-basin, Northwest Australia: insights from quantitative basin modeling. *Mar. Petrol. Geol.* 23 (4), 503–526. <https://doi.org/10.1016/j.marpetgeo.2006.02.005>.
- Cartwright, J.A., 1994. Episodic basin-wide hydrofracturing of overpressured early cenozoic mudrock sequences in the North Sea Basin. *Mar. Petrol. Geol.* 11, 587–607. [https://doi.org/10.1016/0264-8172\(94\)90070-1](https://doi.org/10.1016/0264-8172(94)90070-1).
- Cartwright, J.A., James, D.M.D., Bolton, A.J., 2003. The genesis of polygonal fault systems: a review. In: Van Rensbergen, P., Hillis, R., Morley, C. (Eds.), *Subsurface Sediment Mobilisation*, vol. 216. Geological Society of London, Special Publication. <https://doi.org/10.1144/GSL.SP.2003.216.01.15>, 223–242.
- Chongzhi, T., Guoping, B., Junlan, L., Chao, D., Xiaoxin, L., Houwu, L., Dapeng, W., 2013. Mesozoic lithofacies palaeogeography and petroleum prospectivity in North Carnarvon basin, Australia. *J. Palaeogeogr.* 81–92. <https://doi.org/10.3724/SP.J.1261.2013.00019>.
- Driscoll, N.W., Karner, G.D., 1998. Lower crustal extension across the Northern Carnarvon Basin, Australia: evidence for an eastward dipping detachment. *J. Geophys. Res.* 103, 4975–4991. <https://doi.org/10.1029/97JB03295>.
- Ellis, G., 1987. Lower Cretaceous Radiolarian Biostratigraphy and Depositional Environment of the Windalia Radiolarite, Carnarvon Basin, Western Australia. Honours Thesis, University of Western Australia, unpublished.
- Ercilla, G., Juan, C., Hernandez-Molina, F.J., Bruno, M., Estrada, F., Alonso, B., Casas, D., Lf Farran, M., Llave, E., Garcia, M., 2016. Significance of bottom currents in deep-sea morphodynamics: an example from the alboran sea. *Mar. Geol.* 378, 157–170. <https://doi.org/10.1016/j.margeo.2015.09.007>.
- Etheridge, M.A., O'Brien, G.W., 1994. Structural and tectonic evolution of the Western Australian margin basin system. *PESA J.* 22, 45–64.
- Exon, N.F., Willcox, J.B., 1978. Geology and petroleum potential of Exmouth Plateau area off western Australia. *AAPG Bull.* 62, 10–72. <https://doi.org/10.1306/C1EA47F2-16C9-11D7-8645000102 C1865D>.
- Falvey, D.A., Veevers, J.J., 1974. Physiography of the Exmouth and scott plateaus, western Australia, and adjacent northeast wharton basin. *Mar. Geol.* 17, 21–59. [https://doi.org/10.1016/0025-3227\(74\)90046-2](https://doi.org/10.1016/0025-3227(74)90046-2).
- Gartrell, A.P., 2000. Rheological controls on extensional styles and the structural evolution of the northern Carnarvon Basin, North West Shelf, Australia. *Aust. J. Earth Sci.* 47, 231–244. <https://doi.org/10.1046/j.1440-0952.2000.00776.x>.
- Gartrell, A., Torres, J., Dixon, M., Keep, M., 2016. Mesozoic rift onset and its impact on the sequence stratigraphic architecture of the Northern Carnarvon Basin. *APPEA J* 56, 143–158. <https://doi.org/10.1071/AJ15012>.
- Geoscience Australia, 2015. Regional Geology of the Northern Carnarvon Basin [WWW Document]. *Offshore Pet. Explor. Acreage Release*.
- Gibbons, A.D., Barckhausen, U., Van Den Bogaard, P., Hoernle, K., Werner, R., Whittaker, J.M., Müller, R.D., 2012. Constraining the Jurassic extent of Greater India: tectonic evolution of the West Australian margin. *G-cubed* 13, 1–25. <https://doi.org/10.1029/2011GC003919>.
- Gibbons, A.D., Zahirovic, S., Müller, R.D., Whittaker, J.M., Yatheesh, V., 2015. A tectonic model reconciling evidence for the collisions between India, Eurasia and intra-oceanic arcs of the central-eastern Tethys. *Gondwana Res.* <https://doi.org/10.1016/j.gr.2015.01.001>.
- Heath, R.S., Apthorpe, M.C., 1984. New formation names for the late cretaceous and tertiary sequence of the southern North West Shelf. *GSWA, Record* 1984/7, 35.
- Heine, C., Müller, R.D., 2005. Late Jurassic rifting along the Australian North West Shelf: margin geometry and spreading ridge configuration. *Aust. J. Earth Sci.* 52, 27–39. <https://doi.org/10.1080/08120090500100077>.
- Hengesh, J., Dirstein, J., Stanley, A., 2012. Seafloor geomorphology and submarine landslide hazards along the continental slope in the Carnarvon Basin, Exmouth Plateau, North West Shelf, Australia. *The APPEA Journal* 52, 493–511. <https://doi.org/10.1071/AJ11039>.
- Hernández-Molina, F.J., Llave, E., Somoza, L., Fernández-Puga, M.C., Maestro, A., León, R., Barnolas, A., Medialdea, T., García, M., Vázquez, J.T., Díaz del Río, V., Fernández-Salas, L.M., Lobo, F., Alveirinho Dias, J.M., Roderio, J., Gardner, J., 2003. Looking for clues to paleoceanographic imprints: a diagnosis of the gulf of Cadiz contourite depositional systems. *Geology* 31 (1), 19–22.
- Hernández-Molina, F.J., Larter, R.D., Rebesco, M., Maldonado, A., 2006. Miocene reversal of bottom water flow along the Pacific Margin of the Antarctic Peninsula: stratigraphic evidence from a contourite sedimentary tail. *Mar. Geol.* 228, 93–116. <https://doi.org/10.1016/j.margeo.2005.12.010>.
- Hernández-Molina, F.J., Stow, D.A.V., Llave, 2008. Continental slope contourites. In: Rebesco, M., Camerlenghi, A. (Eds.), *Contourites. Developments in Sedimentology*, 60. Elsevier, Amsterdam, pp. 379–408. [https://doi.org/10.1016/S0070-4571\(08\)10019-X](https://doi.org/10.1016/S0070-4571(08)10019-X).
- Imbert, P., Ho, S., 2012. Seismic-scale funnel-shaped collapse features from the Paleocene-Eocene of the North West Shelf of Australia. *Mar. Geol.* 332, 198–221. <https://doi.org/10.1016/j.margeo.2012.10.010>.
- Jablonski, D., 1997. Recent advances in the sequence stratigraphy of the triassic to lower cretaceous succession in the northern Carnarvon Basin, Australia. *APPEA J* 37, 429–454. <https://doi.org/10.1071/AJ96026>.
- Jablonski, D., Saitta, A.J., 2004. Permian to Lower Cretaceous plate tectonics and its impact on the tectono-stratigraphic development of the western Australian margin. *The APPEA Journal* 44 (1), 287–327. <https://doi.org/10.1071/AJ03011>.
- Keep, M., Harrowfield, M., Crowe, W., 2007. The Neogene tectonic history of the North West Shelf, Australia. *Explor. Geophys.* 38, 151–174.
- Longley, I.M., Buessenschuett, C., Clydsdale, L., Cubitt, C.J., Davis, R.C., Johnson, M.K., Marshall, N.M., Murray, A.P., Somerville, R., Spry, T.B., Thompson, N.B., 2002. The North West shelf of Australia - a worldwide perspective. In: Keep, M., Moss, S. (Eds.), *The Sedimentary Basins of Western Australia 3. Proceedings of the Petroleum Exploration Society of Australia Symposium*, pp. 27–88.
- Marshall, N.G., Lang, S.C., 2013. A new sequence stratigraphic framework for the North West Shelf, Australia. In: Keep, M., Moss, S.J. (Eds.), *The Sedimentary Basins of Western Australia 4. Proceedings of the Petroleum Exploration Society of Australia Symposium*, pp. 1–32.
- Maselli, V., Iacopini, D., Ebbing, C.J., Tewari, S., de Haas, H., Wade, B.S., Pearson, P.N., Francis, M., van Vliet, A., Richards, B., Kroon, D., 2020. Large-scale mass wasting in the western Indian Ocean constrains onset of East African rifting. *Nat. Commun.* 11, 3456.
- Masson, D.G., Wynn, R.B., Bett, B.J., 2004. Sedimentary environment of the Faroe-Shetland and Faroe Bank channels, north-east Atlantic, and the use of bedforms as indicators of bottom current velocity in the deep ocean. *Sedimentology* 51, 1207–1241. <https://doi.org/10.1111/j.1365-3091.2004.00668.x>.
- McCormack, K., McClay, K., 2013. Structural architecture of the gorgan platform, North West Shelf, Australia. In: Keep, M., Moss, S.J. (Eds.), *The Sedimentary Basins of Western Australia IV: Proceedings of the Petroleum Exploration Society of Australia Symposium*. Perth, WA, 2013.
- Metcalfe, I., 2013. Gondwana dispersion and Asian accretion: tectonic and palaeogeographic evolution of eastern Tethys. *J. Asian Earth Sci.* 66, 1–33. <https://doi.org/10.1016/j.jseas.2012.12.020>.
- Miller, K.G., Wright, J.D., Fairbanks, R.G., 1991. Unlocking the ice house: oligocene-miocene 861 oxygen isotopes, eustasy, and margin erosion. *J. Geophys. Res. Solid Earth* 862 96, 6829–6848.
- Mitchum, R.M., Vail, P.R., Sangree, J.B., 1977a. Seismic stratigraphy and global changes of sea-level, part 6: stratigraphic interpretation of seismic reflection patterns in depositional sequences. In: Payton, C.E. (Ed.), *Seismic Stratigraphy - Applications to Hydrocarbon Exploration*, vol. 26. AAPG Memoir, pp. 117–133.
- Mitchum, R.M., Vail, P.R., Thompson, S., 1977b. Seismic stratigraphy and global changes of sea-level, part 2: the depositional sequence as a basic unit for stratigraphic analysis. In: Payton, C.E. (Ed.), *Seismic Stratigraphy - Applications to Hydrocarbon Exploration*, vol. 26. AAPG Memoir, pp. 53–62.
- Moss, G.D., Cathro, D.L., Austin Jr., J.A., 2004. Sequence biostratigraphy of prograding clinoforms, northern Carnarvon Basin, Western Australia: a proxy for variations in Oligocene to Pliocene global sea level? *Palaios* 19, 206–226. [https://doi.org/10.1669/0883-1351\(2004\)019 <0206:SBOPCN>2.0.CO](https://doi.org/10.1669/0883-1351(2004)019 <0206:SBOPCN>2.0.CO).

- Müller, R.D., Mihut, D., Baldwin, S., 1998. A new kinematic model for the formation and evolution of the West and Northwest Australian Margin. In: Purcell, P.G., Purcell, R.R. (Eds.), *The Sedimentary Basins of Western Australia 2. Proceedings of the Petroleum Exploration Society of Australia Symposium*. Perth, WA, pp. 56–72.
- Nugraha, H.D., Jackson, C.A.-L., Johnson, H.D., Hodgson, D.M., Reeve, M.T., 2019. Tectonic and oceanographic process interactions archived in the Late Cretaceous to Present deep-marine stratigraphy on the Exmouth Plateau, offshore NW Australia. *Basin Res.* 31, 405–430. <https://doi.org/dbgw.lis.curtin.edu.au/10.1111/bre.12328>.
- Norvick, M.S., 2002. Palaeogeographic Maps of the Northern Margins of the Australian Plates: Initial Report (Unpublished report for Geoscience Australia).
- Pattillo, J., Nichols, P.J., 1990. A tectonostratigraphic framework for the Vulcan graben, Timor Sea region. *APEA J.* 30, 27–51.
- Paumard, V., Bourget, J., Payenberg, T., Ainsworth, R.B., George, A.D., Lang, S., Posamentier, H.W., Peyrot, D., 2018. Controls on shelf-margin architecture and sediment partitioning during a syn-rift to post-rift transition: insights from the Barrow Group (northern Carnarvon Basin, North West Shelf, Australia). *Earth-Science Reviews* Volume 177, 643–677. <https://doi.org/10.1016/j.earscirev.2017.11.026>. February 2018.
- Paumard, V., Bourget, J., Lang, S., Wilson, T., Riera, R., Gartrell, A., Vakarelov, B., O'Leary, M., George, A.D., 2019. Imaging past depositional environments of the North West Shelf of Australia: lessons from 3D seismic data. In: Keep, M., Moss, S.J. (Eds.), *The Sedimentary Basins of Western Australia V: Proceedings of the Petroleum Exploration Society of Western Australia Symposium*. Perth, WA, p. 30, 2019.
- Payenberg, T.H.D., Howe, H., Marsh, T., Sixsmith, P., Kowalik, W.S., Powell, A., Ratcliffe, K., Iasky, V., Allgoewer, A., Howe, R.W., Montgomery, P., Vonk, A., Croft, M., 2013. 2013—An Integrated regional Triassic stratigraphic framework for the Carnarvon Basin, NWS, Australia. In: Keep, M., Moss, S.J. (Eds.), *The Sedimentary Basins of Western Australia IV: Proceedings of the Petroleum Exploration Society of Australia Symposium*. Perth, WA.
- Rebesco, M., Stow, D.A.V., 2001. Seismic expression of contourites and related deposits: a preface. *Mar. Geophys. Res.* 22, 303–308. <https://doi.org/10.1023/A:1016316913639>.
- Rebesco, M., 2005. Contourites. In: Selley, R.C., Cocks, L.R.M., Plimer, I.R. (Eds.), *Encyclopedia of Geology*. Elsevier, Oxford, pp. 513–527.
- Rebesco, M., Hernández-Molina, J., van Rooij, D., Wählin, A., 2014. Contourites and associated sediments controlled by deep-water circulation processes: state-of-the-art and future considerations. *Mar. Geol.* 352, 111–154. <https://doi.org/10.1016/j.margeo.2014.03.011>.
- Reeve, M.T., Jackson, C.A.L., Bell, R.E., Magee, C., Bastow, I.D., 2016. The stratigraphic record of prebreakup geodynamics: evidence from the Barrow Delta, offshore Northwest Australia. *Tectonics* 35, 1935–1968.
- Romine, K.K., Durrant, J.M., Cathro, D.L., Bernardel, G., 1997. Petroleum play element prediction for the Cretaceous-Tertiary basin phase, Northern Carnarvon Basin. *APPEA J* 37, 315–339. <https://doi.org/10.1071/AJ96020>.
- Sanchez, M.C., Fulthorpe, S.C., Steel, J.R., 2012. Middle Miocene–Pliocene Siliciclastic Influx across a Carbonate Shelf and Influence of Deltaic Sedimentation on Shelf Construction, Northern Carnarvon Basin, Northwest Shelf of Australia. *Basin Research*. Blackwell Publishing Ltd, European Association of Geoscientists & Engineers and International Association of Sedimentologists, pp. 1–19. <https://doi.org/10.1111/j.1365-2117.2012.00546.x>, 24.
- Scarselli, N., McClay, K., Elders, C., 2013. Submarine slide and slump complexes, Exmouth Plateau, NW shelf of Australia. In: Keep, M., Moss, S.J. (Eds.), *Western Australian Basins Symposium 2013, Aug 18-21 2013*. Perth: Petroleum Exploration Society of Australia. <https://doi.org/10.1002/9781119500513.ch16>.
- Scarselli, N., McClay, K.R., Elders, C., 2020. Seismic examples of composite slope failures (offshore North West Shelf, Australia). In: Ogata, K., Pini, G.A., Festa, A. (Eds.), *Submarine Landslides: Subaqueous Mass Transport Deposits from Outcrops to Seismic Profiles*, vol. 246. AGU Geophysical Monograph Series. <https://doi.org/10.1002/9781119500513.ch16>.
- Stagg, H.M.J.G.J., Colwell, J.B., 1994. *The structural foundations of the northern Carnarvon Basin*. *Sediment. Basins west. Aust. Proc. Pet. Explor. Soc. Aust. Symp.* 349–364. Perth 1994.
- Stow, D.A.V., Kahler, G., Reeder, M., 2002. Fossil contourites: type example from an Oligocene palaeoslope system, Cyprus. In: Stow, D.A.V., Pudsey, C.J., Howe, J.A., Faugères, J.-C., Viana, A.R. (Eds.), *Deep-water Contourite Systems: Modern Drifts and Ancient Series, Seismic and Sedimentary Characteristics*, vol. 22. Geological Society, London, Memoir, pp. 443–455. <https://doi.org/10.1144/GSL.MEM.2002.022.01.31>.
- Stow, D.A.V., Hernández-Molina, F.J., Llave, E., Sayago-Gil, M., Díaz-del Río, V., Branson, A., 2009. Bedform-velocity matrix: the estimation of bottom current velocity from bedform observations. *Geology* 37, 327–330. <https://doi.org/10.1130/G25259A.1>.
- Tindale, K., Newell, N., Keall, J., Smith, N., 1998. Structural evolution and charge history of the Exmouth Sub-basin, northern Carnarvon Basin, western Australia. In: Purcell, P.G., Purcell, R.R. (Eds.), *The Sedimentary Basins of Western Australia 2. Proceedings of the Petroleum Exploration Society of Australia Symposium*, pp. 447–472.
- Tellez, J.J., 2015. *Seismic Sequence Stratigraphy and Architectural Elements for Cenozoic Strata at the Rankin Platform Sub-Basin, North Carnarvon Basin, Australia*. In: Master Thesis, vol. 108. The University of Oklahoma.
- Tortopoglu, B., 2015. *The Structural Evolution of the Northern Carnarvon Basin, Northwest Australia*. Master Thesis. University of Colorado School of Mines, p. 170.
- Veevers, J.J., 2000. Change of tectono-stratigraphic regime in the Australian plate during the 99 Ma (mid-Cretaceous) and 43 Ma (mid-Eocene) swerves of the Pacific. *Geology* 28 (1), 47–50.
- Watterson, J., Walsh, J.J., Nicol, A., Nell, R.R., Breatan, P.G., 2000. Geometry and origin of a polygonal fault system. *J. Geol. Soc. Lond.* 157, 151–162. <https://doi.org/10.1144/jgs.157.1.151>.
- Whittam, D.B., Norvick, M.S., McIntyre, C.L., 1996. Mesozoic and Cainozoic tectonostratigraphy of western ZOCA and adjacent areas. *APPEA J* 36, 209–232.